

YOUNGSTOWN STATE UNIVERSITY

Graduate School

THESIS

Submitted in Partial Fulfillment of the Requirements

For the Degree of Master of Science

TITLE PHOTOELECTROCHEMISTRY WITH POLYMER SEMICONDUCTORS:
POLY(CHROME AZUROL S-ACETYLENE)

PRESENTED BY Alan J. Oleksa

ACCEPTED BY THE DEPARTMENT OF Chemistry

Howard J. Motter

August 15, 1982

Major Professor

Date

Daryl W. Minney

Aug 15, 1982

Date

** Steven M. Schilderout*

August 15, 1982

Date

Sally M. Hitchkiss

August 19, 1982

Dean, Graduate School

Date

WILLIAM F. MAAG LIBRARY
YOUNGSTOWN STATE UNIVERSITY

ACKNOWLEDGMENTS

I would like to thank Dr. Edward D. Matias whose

PHOTOELECTROCHEMISTRY WITH POLYMER SEMICONDUCTORS :

guidance and understanding made this thesis possible.

POLY(CHROME AZUROL S-ACETYLENE)

I would also like to extend my appreciation to

Dr. Daryl Mincey and Dr. Stephen Schilderout for their

Alan J. Oleksa

time and effort reviewing the manuscripts.

Master of Science

Youngstown State University, 1982

The present work is concerned with producing a polymer semiconductor which could photocatalyze the decomposition of water. The method chosen to couple an acetylene, (conductive polymer), to an organic dye, (light absorber), was the Williamson ether synthesis. If polymerized, the intention was that the polymer would be conductive, while the organic dye would branch off the polymer as a "pendent" group and be a necessary ingredient for an electrical gradient, separating a charge and producing a chemical potential, when light illuminated the polymer.

The structure of the "dye derivatized" acetylene was confirmed with the use of nmr, ir, and TLC data. Cyclic voltammetry was employed as a tool in determining any electroactive species in the dye. The cyclic voltammograms confirmed the presence of a conductive layer on the surface of the electrode, consistent with that of electropolymerizations, but was unstable upon exposure to air, and wouldn't conduct when reimmersed in electrolyte solution.

ACKNOWLEDGEMENTS

I would like to thank Dr. Howard D. Mettee whose guidance and understanding made this thesis possible.

I would also like to extend my appreciation to Dr. Daryl Mincey and Dr. Stephen Schildcrout for their time and effort reviewing the manuscripts.

ABSTRACT	11
ACKNOWLEDGEMENTS	111
TABLE OF CONTENTS	iv
LIST OF SYMBOLS	vi
LIST OF FIGURES	vii
LIST OF TABLES	ix
CHAPTER	
I. INTRODUCTION	1
General	1
Band Theory of Semiconductors	2
Semiconductor Theory of Photoelectro-chemistry	7
Water Decomposition	13
Statement of the Problem	15
II. REVIEW OF THE LITERATURE	19
Polyacetylene as a Backbone	19
Conductivity of Polyacetylene	19
Theory of Conductivity	21
III. EXPERIMENTAL	27
Materials and Apparatus	27
Chemistry of Chrome Azurol S	28
Williamson Ether Synthesis	28
Thin Layer Chromatography	30
Infrared Data	30

TABLE OF CONTENTS

	PAGE
ABSTRACT	ii
ACKNOWLEDGEMENTS	iii
TABLE OF CONTENTS	iv
LIST OF SYMBOLS	vi
LIST OF FIGURES	vii
LIST OF TABLES	ix
CHAPTER	
I. INTRODUCTION	1
General	1
Band Theory of Semiconductors	2
Semiconductor Theory of Photoelectro-chemistry	7
Water Decomposition	13
Statement of the Problem	15
II. REVIEW OF THE LITERATURE	19
Polyacetylene as a Backbone	19
Conductivity of Polyacetylene	19
Theory of Conductivity	21
III. EXPERIMENTAL	27
Materials and Apparatus	27
Chemistry of Chrome Azurol S	28
Williamson Ether Synthesis	28
Thin Layer Chromatography	30
Infrared Data	30

LIST OF SYMBOLS		PAGE
SYMBOL	Nuclear Magnetic Resonance	UNITS 31
C_b	Cyclic Voltammetry	31
IV.	RESULTS AND DISCUSSION	34
e^-	Monomer Evidence	34
h^+	Williamson Ether Synthesis	34
E_f	Thin Layer Chromatography	eV 34
E_{fb}	Infrared Data	eV 35
E_f	Nuclear Magnetic Resonance	eV 38
μA	Cyclic Voltammetry	10^{-6} 43
V.	CONCLUSIONS	53
BIBLIOGRAPHY	55
S^0	Neutral soliton	
S^+	Positively charged soliton	
S^-	Negatively charged soliton	
ρ	Resistivity	$\text{ohm}\cdot\text{cm}$
σ	Conductivity	$(\text{ohm}\cdot\text{cm})^{-1}$
E_g	Band gap potential	eV
$(CH)_x$	Polyacetylene; also poly(CH)	
PEC	Photoelectrochemical	
CV	Cyclic voltammetry	
v	Scan rate	mV/sec
16.	
17.	
18.	
19.	

LIST OF SYMBOLS

SYMBOL	DEFINITION	UNITS
C_b	Conduction band	
V_b	Valence band	
e^-	electron	
h^+	hole	
E_g	Band gap Between the Valence and Conduction Band Intrinsic Semiconductor	eV
E_{fb}	Flat band potential P-type Extrinsic Semiconductors	eV
E_0^+	Standard potential of redox couple	eV
μA	Microamperes	10^{-6} amps
Ox	Oxidized species of redox couple	
Red	Reduced species of redox couple	
S^0	Neutral soliton	
S^+	Positively charged soliton	
S^-	Negatively charged soliton	
ρ	Resistivity	ohm·cm
σ	Conductivity	(ohm·cm) ⁻¹
E_g	Band gap potential	eV
$(CH)_x$	Polyacetylene; also poly(CH)	
PEC	Photoelectrochemical	
CV	Cyclic voltammetry	
v	Scan rate	mV/sec

FIGURE	LIST OF FIGURES	PAGE
FIGURE	Effects Donors Have on Solitons	PAGE
21.	Color Transformation of CAS	29
1.	Diagram of How Energy Levels in an Atom Become Energy Bands in a Group of Atoms	3
2.	Energy Bands for an Insulator, a Metal, and an Intrinsic Semiconductor	3
3.	Band Gap Between the Valence and Conduction Bands in an Intrinsic Semiconductor	6
4.	Energy Bands of N- and P-type Extrinsic Semiconductors	6
5.	Resistivity Versus Temperature in a Doped Semiconductor	8
6.	Energy Relation Within a Semiconductor/Elec- trolyte Interface	8
7.	Fermi Level in an N-type Semiconductor Before and After Immersion in a Redox Solution	10
8.	Effects of Illumination on the Depletion Layer in N- and P-type Semiconductors	10
9.	Photovoltage Diagram	12
10.	Current Versus Voltage for an N-type Semi- conductor in the Dark and Illuminated	12
11.	Diagram for Minimum Conditions Required for Water Decomposition	14
12.	An N-P Photoassisted System	14
13.	Photosystems I and II	16
14.	Structure of Chrome Azurol S	16
15.	The Williamson Ether Synthesis	18
16.	Isomeric Forms of $(CH)_x$	22
17.	Defects Caused by the Soliton Domain	23
18.	Migration of Solitons and Their Annihilation ...	23
19.	Effects Acceptors Have on the Solitons	26

FIGURE	LIST OF TABLES	PAGE
20.	Effects Donors Have on Solitons	26
21.	Color Transformation of CAS	29
22.	Apparatus for the Williamson Ether Synthesis ...	29
23.	Illustration of a Cyclic Voltammogram	33
24.	IR Spectrum of KBr Pellet	36
25.	IR Spectrum of CAS	37
26.	NMR Spectrum of CAS	39
27.	NMR Spectrum of the Monomer	40
28.	NMR Spectrum of Propargyl Bromide	41
29.	Cyclic Voltammogram of CAS, .1N Na ₂ SO ₄ , and the Monomer	44
30.	Cyclic Voltammogram of the Monomer Cycled for 1 Hour	45
31.	Cyclic Voltammogram of Coated Pt Electrode _o that was removed	46
32.	Results of Current Versus Scan Rates	48
33.	Cyclic Voltammogram of the Monomer Solution in the Dark and Illuminated	50
34.	Cyclic Voltammogram of a Poised Electrode	51

LIST OF TABLES

TABLE	CHAPTER I	PAGE
1.	Comparisons of Conductivity	20
2.	Bands in Infrared Analysis	35
3.	NMR Peaks of CAS	38
4.	NMR Peaks of Derviatized CAS	42
5.	Anodic Current Versus Scan Rate for the Monomer .	47

One use of conducting polymers is to employ solar energy to split water into oxygen and hydrogen, where hydrogen could be a useful source of energy on earth. One conductive polymer of interest in this thesis is polyacetylene, $(CH)_x$, whose properties may aid in photoelectrochemistry. As Mettes¹ states, polymers may play a central role in light absorption, charge separation, and particle flow dynamics that make up part of the photoelectrochemical (PEC) process.

"The solar energy coming down onto the earth's surface amounts to ca. 3×10^{24} J per year, which is about 10^4 times the world-wide yearly energy consumption."²

Why not harness some of the sun's radiant energy? For systems converting solar energy into electrical, Watanabe³ has elaborated on two criteria. First, there has to be absorption by a "chemical substance" of solar energy which would be able to cause the separation of electron (e^-)-hole (h^+) pairs. The second factor to consider is to separate these e^-/h^+ pairs with minimum loss due to recombination.

CHAPTER I

INTRODUCTION

General

Conducting polymers have opened a new field in photoelectrochemistry whose potential has yet to be exploited. One use of conducting polymers is to employ solar energy to split water into oxygen and hydrogen, where hydrogen could be a useful source of energy on earth. One conductive polymer of interest in this thesis is polyacetylene, $(CH)_x$, whose properties may aid in photoelectrochemistry. As Mettee¹ states, polymers may play a central role in light absorption, charge separation, and particle flow dynamics that make up part of the photoelectrochemical (PEC) process.

"The solar energy coming down onto the earth's surface amounts to ca. 3×10^{24} J per year, which is about 10^4 times the world-wide yearly energy consumption."²

Why not harness some of the sun's radiant energy? For systems converting solar energy into electrical, Watanabe³ has elaborated on two criteria. First, there has to be absorption by a "chemical substance" of solar energy which would be able to cause the separation of electron (e^-)-hole (h^+) pairs. The second factor to consider is to separate these e^-/h^+ pairs with minimum loss due to recombination.

tion bands (C_p), corresponding to the Homo and Lumo levels

In order that this charge separation proceeds effectively, there should be a potential gradient established where this excitation takes place. It was pointed out that a way to create a potential gradient is by "band bending" in a semiconductor material at the interface of a liquid junction. When a semiconductor is used as an electrode, and it is connected to a counter electrode, photoexcitation of the semiconductor can generate a chemical potential to cause a redox reaction on the surface of the electrode. Another example of such an interface is the lipid membrane of the chloroplast of green plants, which is a very economic and durable form of solar converter.

Band Theory of Semiconductors

Energy bands originate in semiconductors when atoms are brought into a collection to form a solid. The Pauli Exclusion Principle has to be obeyed, and so discrete atomic levels are formed into bands of levels in the solid, (Figure 1). At absolute zero temperature, lower energy levels are filled first before higher levels so that the upper levels are empty. The highest filled level is known as the valence band (V_b). The Fermi energy (E_f) is characteristic of the chemical potential of electrons in a semiconductor. Holes also have a Fermi level.

Insulators, metals, and semiconductors can be compared by the width of band gap between valence and conduction bands (C_b), corresponding to the Homo and Lumo levels

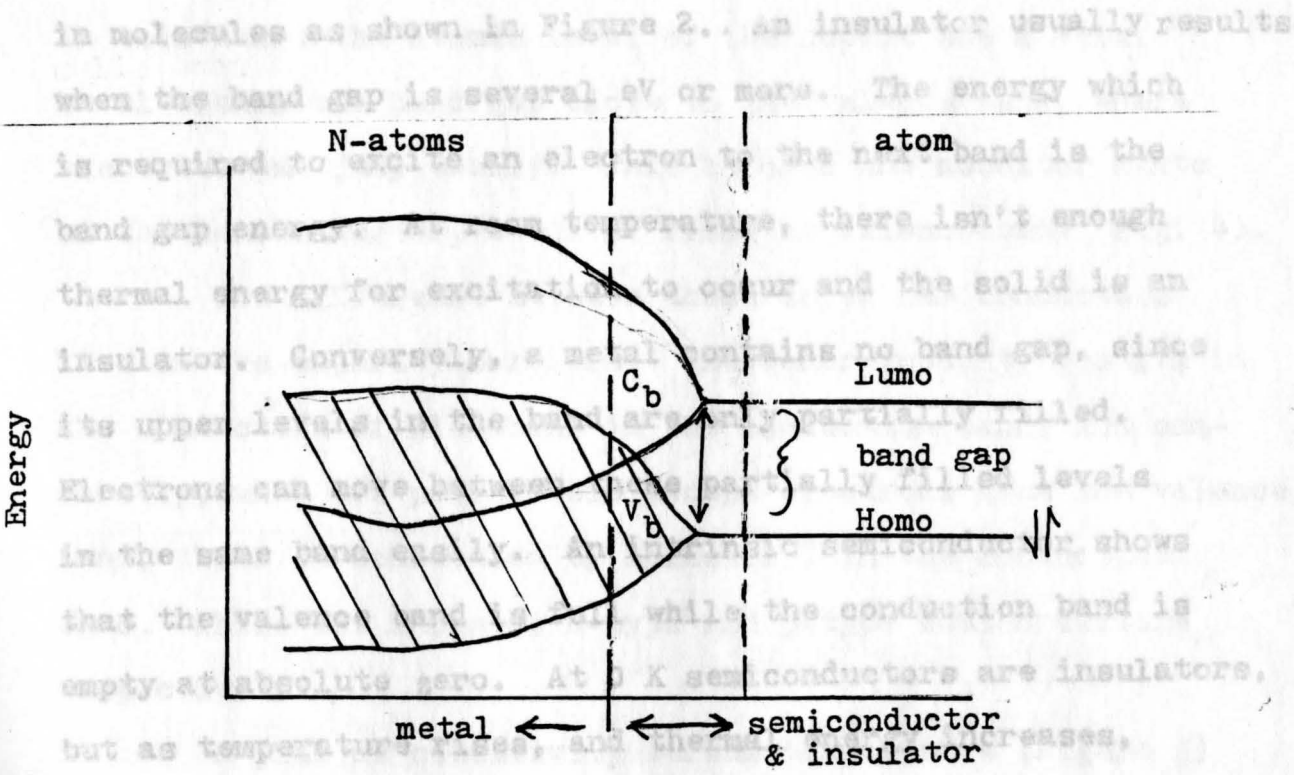


Fig. 1. Energy levels for electrons in the outer shells of a free atom (Right). Energy bands for the electrons in a solid are shown also (Left).

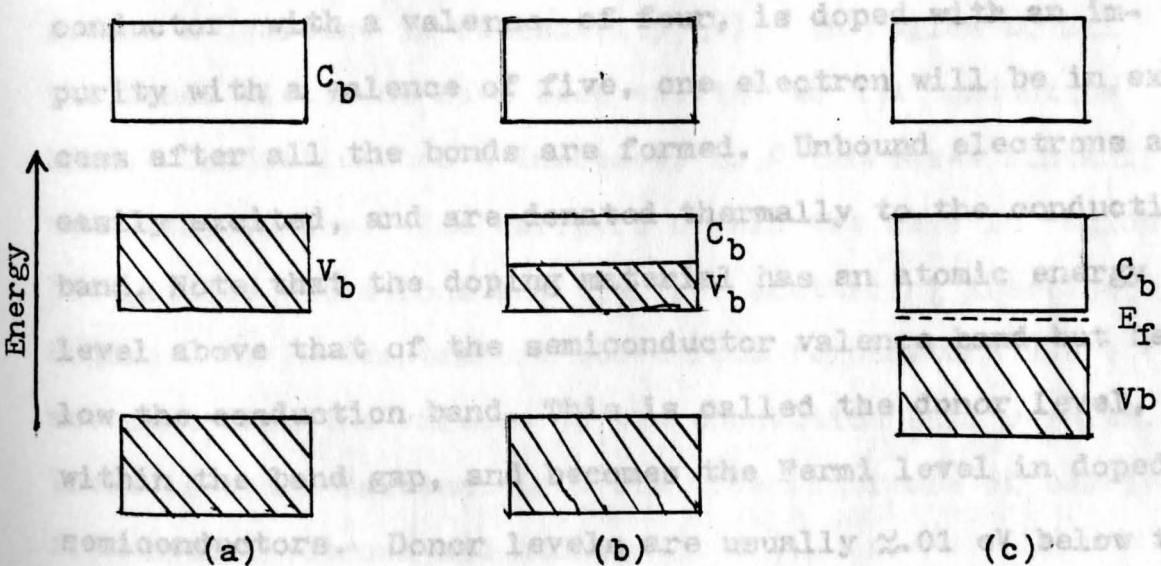


Fig. 2. Energy bands for an insulator, (a), a metal (b), and an intrinsic semiconductor (c).

electron after all the bonds are formed between the atoms.

in molecules as shown in Figure 2. An insulator usually results when the band gap is several eV or more. The energy which is required to excite an electron to the next band is the band gap energy. At room temperature, there isn't enough thermal energy for excitation to occur and the solid is an insulator. Conversely, a metal contains no band gap, since its upper levels in the band are only partially filled. Electrons can move between these partially filled levels in the same band easily. An intrinsic semiconductor shows that the valence band is full while the conduction band is empty at absolute zero. At 0 K semiconductors are insulators, but as temperature rises, and thermal energy increases, electrons are excited from the valence band into the conduction band leaving holes in the valence band. (Figure 3)

When an element such as silicon, an intrinsic semiconductor with a valence of four, is doped with an impurity with a valence of five, one electron will be in excess after all the bonds are formed. Unbound electrons are easily excited, and are donated thermally to the conduction band. Note that the doping material has an atomic energy level above that of the semiconductor valence band but below the conduction band. This is called the donor level, within the band gap, and becomes the Fermi level in doped semiconductors. Donor levels are usually ≈ 0.01 eV below the C_b .

If silicon is doped with an impurity atom with a valence of three, there will be an absence of a bonding electron after all the bonds are formed between the atoms.

In this case, the atomic level of the dopant has a Fermi level within the band gap close to the valence band, where electrons can jump easily. This becomes the acceptor state of the semiconductor, $\approx .01$ eV from the valence band (Fig. 4).

The difference between these doped semiconductors lies in the majority carriers. The donor impurity results in the conduction of electrons in the conduction band, and conversely, when acceptor levels accept electrons from the valence band, there is conduction by holes (h^+) in the conduction band. These are known as n-type and p-type semiconductors, respectively.

A plot of resistivity versus temperature (Figure 5) of an n-type semiconductor, as it is brought from 0 K, shows that region A, about 10 K, has enough energy to empty the donor state electrons into the conduction band. This is seen as a decrease in resistivity (ρ). In region B, all the donor electrons have been excited to the conduction band. Conduction can't increase, so ρ increases linearly with temperature. The carriers remain the same in region B, but lattice vibrations and electron scattering increase ρ . Region C is a temperature above room temperature where e^- movement from the valence to the conduction band results. There is now a decrease in ρ due to an increase of carriers from both electrons and holes.

Fig. 3. Left: band gap between valence and conduction bands. Right: electrons move from the valence band to the conduction band.

Fig. 4. Left: conduction band populated by donor state (E_D) of the n-type semiconductor. Right: conduction band of a p-type semiconductor as a result of electron migration to the conduction band and the acceptor state (E_A).

Semiconductor Theory of Photoelectrochemistry

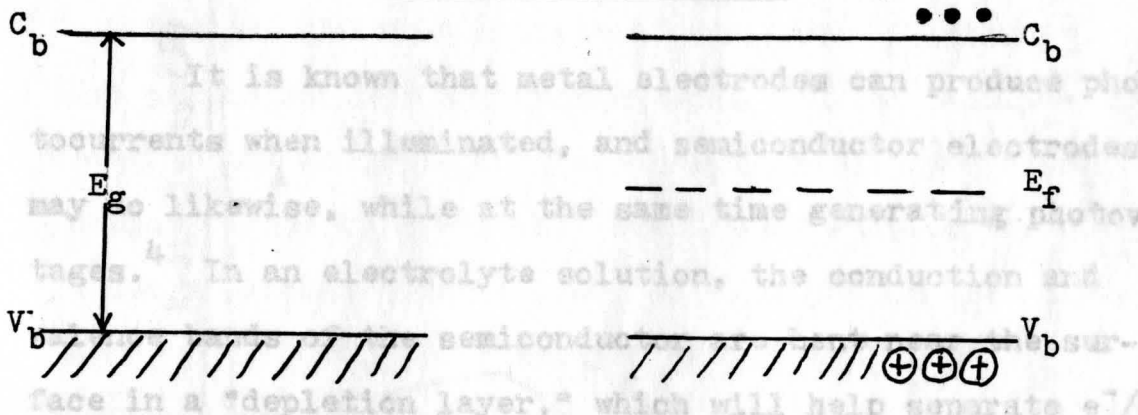
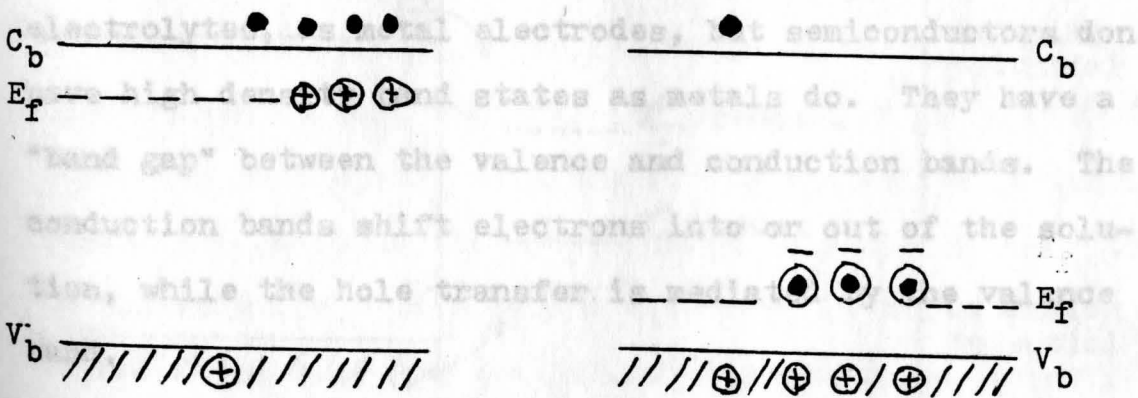


Fig. 3. Left: band gap between valence and conduction bands. Right: electrons move from the valence band to the conduction band in an intrinsic semiconductor.

According to Janssen, photoelectrolysis is the re-

sult of a photoelectric effect combined with "chemical reactivity." Semiconductor electrodes perform redox chemistry in



Electrolysis with solution redox reactions may be

Fig. 4. Left: conduction band populated with electrons from the valence band and the donor state (E_f) of the n-type semiconductor. Right: holes in the conduction band of a p-type semiconductor as a result of electron migration to the conduction band and the acceptor state (E_f).

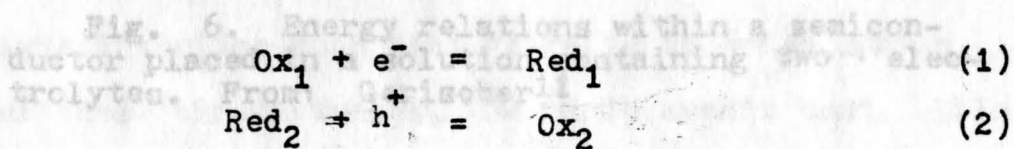
where Ox_1 , Ox_2 , Red_1 , and Red_2 are oxidized and reduced species of the redox couple; e^- is the electron from the

Semiconductor Theory of Photoelectrochemistry

It is known that metal electrodes can produce photocurrents when illuminated, and semiconductor electrodes may do likewise, while at the same time generating photovoltages.⁴ In an electrolyte solution, the conduction and valence bands of the semiconductor are bent near the surface in a "depletion layer," which will help separate e^-/h^+ pairs and thus make the carriers available for conduction and for redox reactions.

According to Janzen,⁵ photoelectrolysis is the result of a photoelectric effect combined with "chemical reactivity." Semiconductor electrodes perform redox chemistry in electrolytes, as metal electrodes, but semiconductors don't have high density band states as metals do. They have a "band gap" between the valence and conduction bands. The conduction bands shift electrons into or out of the solution, while the hole transfer is mediated by the valence band.

Electrolysis with solution redox reactions may be represented as follows:



where Ox_1 , Ox_2 , Red_1 , and Red_2 are oxidized and reduced species of the redox couple; e^- is the electron from the

conduction band; h^+ is the hole of the valence band. When a semiconductor is placed in a solution, the chemical potential of e^- in the semiconductor given by E_F , will differ from that of the redox couple in solution E_F^0 (Figure 6). What occurs is that the Fermi levels will equilibrate by transferring majority carriers, usually into the electrolyte. As equilibrium is attained, there is an accumulation of ions at the electrode surface, (H^+ , OH^-), known as the Helmholtz layer, and there is usually a charge depletion within the surface of the semiconductor. In an n-type material, E_F for the semiconductor is usually less than E_F^0 the redox couple in solution, and electrons flow from the semiconductor, which becomes positively charged at the surface, as shown in Figure 7.

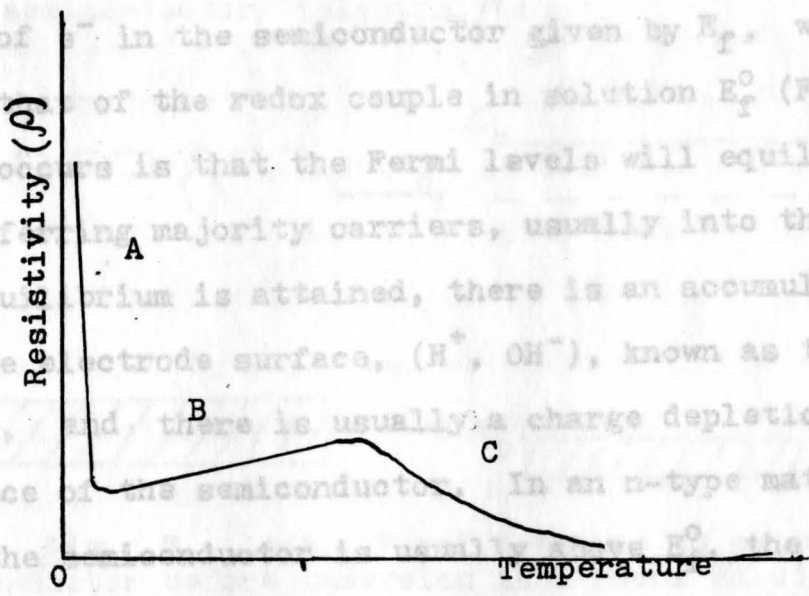


Fig. 5. Resistivity of a doped semiconductor as a function of temperature.

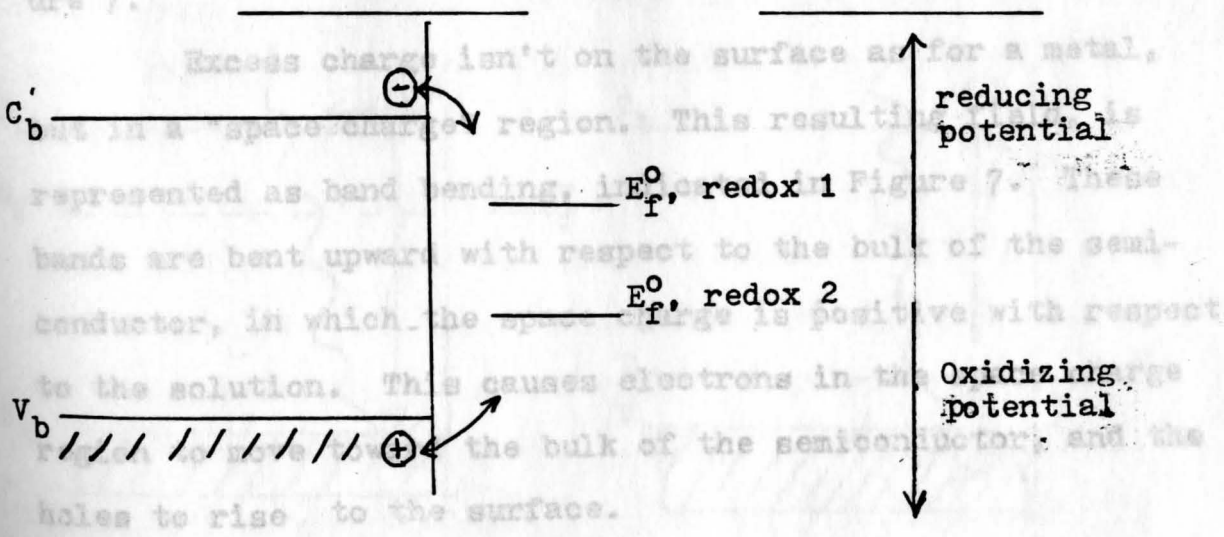


Fig. 6. Energy relations within a semiconductor placed in a solution containing two electrolytes. From: Gerischer¹¹

and under these circumstances, the bands aren't bent. This potential is known as the "flat band potential," (E_{FB}).

It is a unique property of semiconductors, where

conduction band; h^+ is the hole of the valence band. When a semiconductor is placed in a solution, the chemical potential of e^- in the semiconductor given by E_f , will differ from that of the redox couple in solution E_f^0 (Figure 6). What occurs is that the Fermi levels will equilibrate by transferring majority carriers, usually into the electrolyte. As equilibrium is attained, there is an accumulation of ions at the electrode surface, (H^+ , OH^-), known as the Helmholtz layer, and there is usually a charge depletion within the surface of the semiconductor. In an n-type material, E_f for the semiconductor is usually above E_f^0 , the redox couple in solution, and electrons move from the semiconductor, which becomes positive, to the solution, as shown in Figure 7.

Excess charge isn't on the surface as for a metal, but in a "space charge" region. This resulting field, is represented as band bending, indicated in Figure 7. These bands are bent upward with respect to the bulk of the semiconductor, in which the space charge is positive with respect to the solution. This causes electrons in the space charge region to move toward the bulk of the semiconductor, and the holes to rise to the surface.

A potential may be imposed upon the semiconductor/electrolyte interface such that there is no space charge, and under these circumstances, the bands aren't bent. This potential is known as the "flat band potential," (E_{fb}).

It is a unique property of semiconductors, where

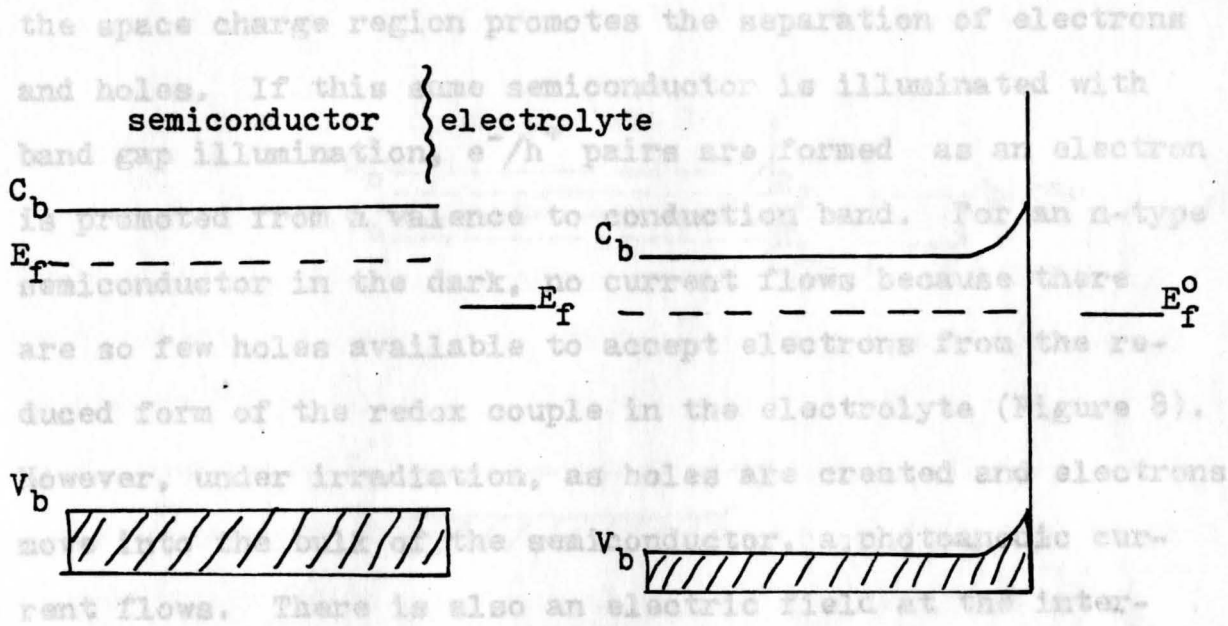


Fig. 7. Left: Fermi level in an n-type semiconductor before immersion in a redox solution. Right: Fermi level after immersion. An electron depletion layer formed within the electrode causing band bending.

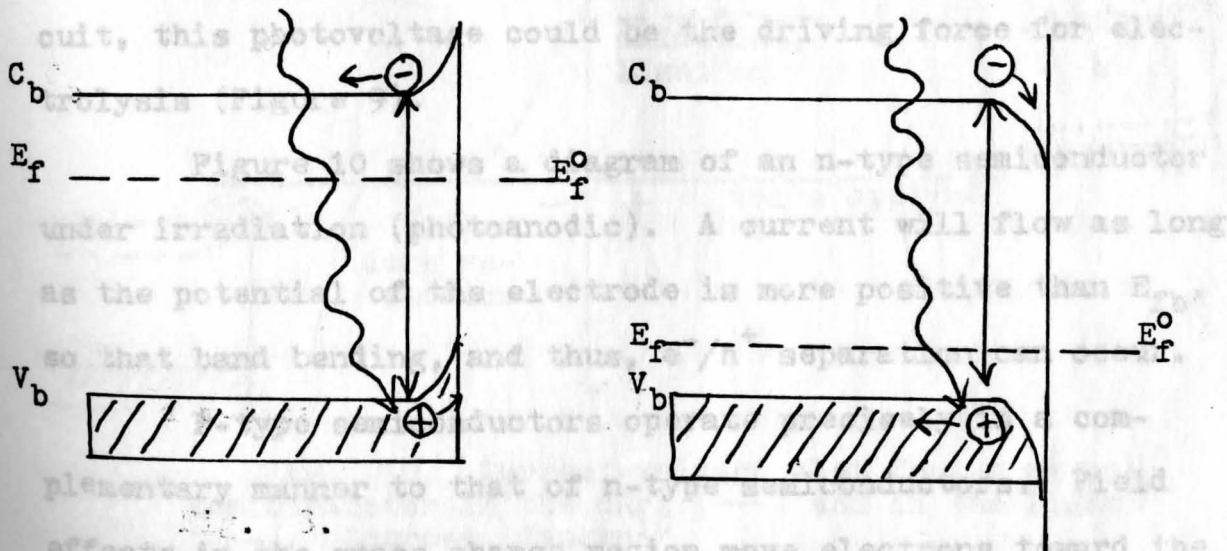


Fig. 8. The effects of illumination in the depletion layer. Left: the effects at the interface of an n-type semiconductor. Right: the electric field separates the charge at the interface of a p-type semiconductor. Source: Gerischer¹¹

in solution.

the space charge region promotes the separation of electrons and holes. If this same semiconductor is illuminated with band gap illumination, e^-/h^+ pairs are formed as an electron is promoted from a valence to conduction band. For an n-type semiconductor in the dark, no current flows because there are so few holes available to accept electrons from the reduced form of the redox couple in the electrolyte (Figure 8). However, under irradiation, as holes are created and electrons move into the bulk of the semiconductor, a photoanodic current flows. There is also an electric field at the interface, causing a shift of the conduction and valence bands upward, diminishing the band bending. The photovoltage is the change in Fermi levels from dark to illuminated conditions, and if a counter electrode were introduced to the circuit, this photovoltage could be the driving force for electrolysis (Figure 9).

Figure 10 shows a diagram of an n-type semiconductor under irradiation (photoanodic). A current will flow as long as the potential of the electrode is more positive than E_{fb} , so that band bending, and thus, e^-/h^+ separation can occur.

P-type semiconductors operate precisely in a complementary manner to that of n-type semiconductors. Field effects in the space charge region move electrons toward the surface and holes toward the bulk (Figure 8), so that p-type materials catalyze photoreductions of redox couples in solution.

Water Decomposition

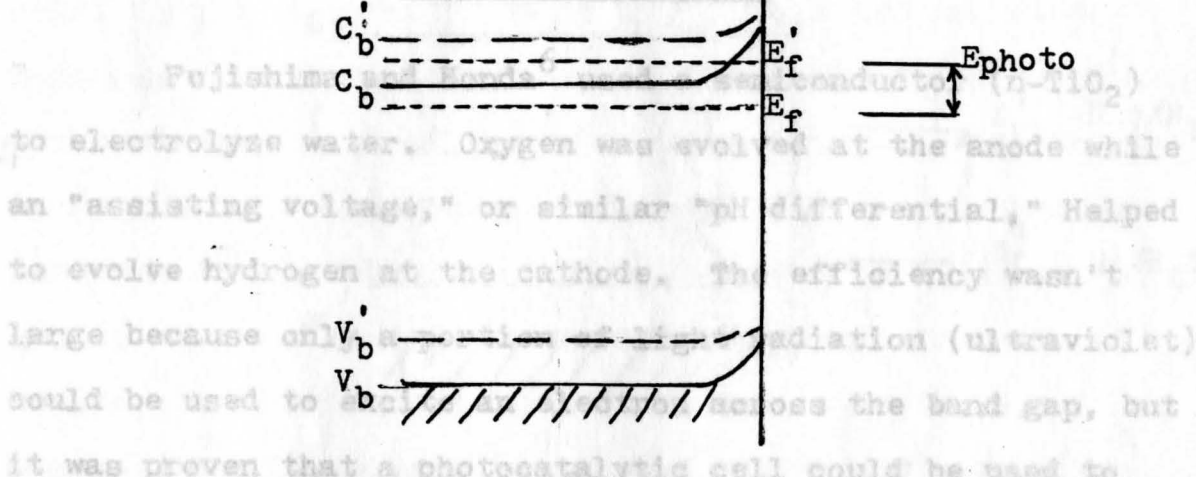


Fig. 9. Illumination produces a counter field which shifts the valence and conduction band upward in the n-type semiconductor. Photovoltage, (E_{photo}), is the change in Fermi level. Source: Gerischer¹²

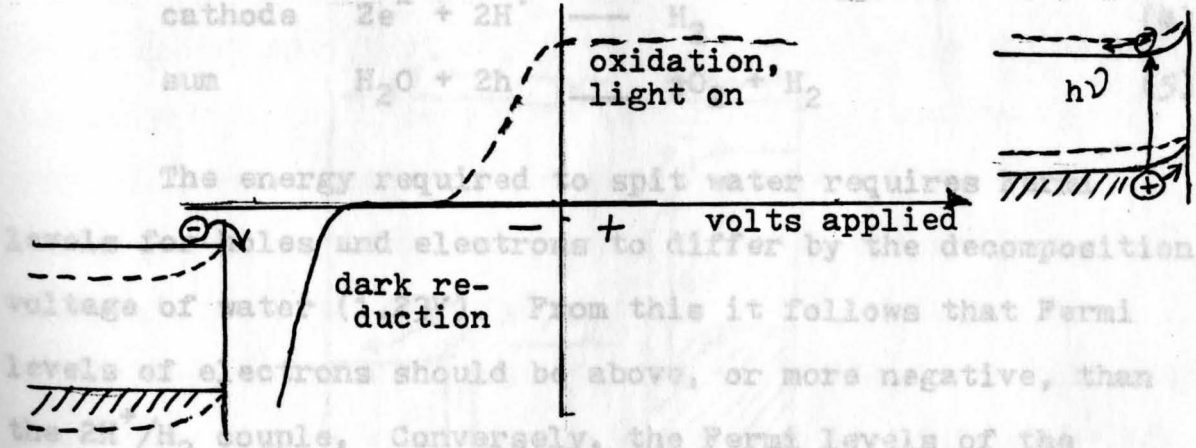
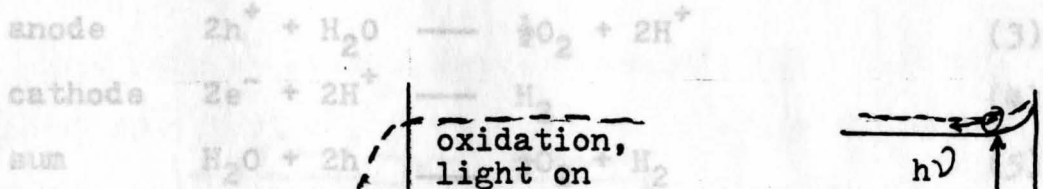
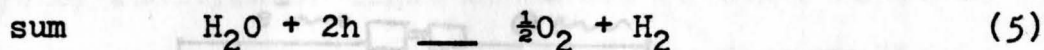
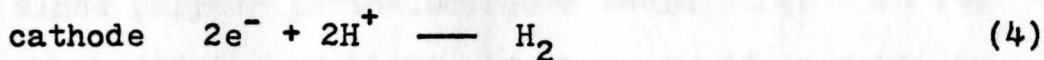
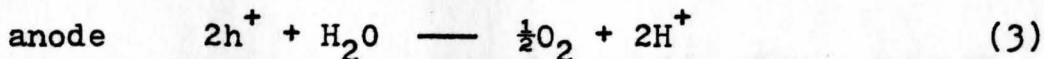


Fig. 10. Current-voltage plot for an n-type semiconductor in the dark (—) and in the light couple (---). Source: Janzen¹⁰

Water Decomposition

Fujishima and Honda⁶ used a semiconductor (n-TiO₂) to electrolyze water. Oxygen was evolved at the anode while an "assisting voltage," or similar "pH differential," helped to evolve hydrogen at the cathode. The efficiency wasn't large because only a portion of light radiation (ultraviolet) could be used to excite an electron across the band gap, but it was proven that a photocatalytic cell could be used to split water.

The reactions could be summarized as follows:



The energy required to split water requires Fermi levels for holes and electrons to differ by the decomposition voltage of water (1.23V). From this it follows that Fermi levels of electrons should be above, or more negative, than the 2H⁺/H₂ couple. Conversely, the Fermi levels of the holes should be below, or more positive, than the H₂O/O₂ couple (Figure 11). Therefore, illumination has to be sufficiently energetic to split Fermi levels of the holes and electrons by more than the decomposition voltage, which would be the minimum energy requirement.

Most semiconductors have too large a band gap to absorb visible light, or are unable to decompose water because Fermi levels can't split enough to cause evolution of hydrogen and oxygen. To overcome this deficiency, Nozik suggested placing two semiconductor photoelectrodes in series: an n-type for O_2 evolution, and the p-type for hydrogen production. The electrodes could produce additive potentials to increase the "overpotential" as shown in Figure 12. This arrangement of two photoelectrodes in series mimics the natural arrangement of Photosystems I and II.

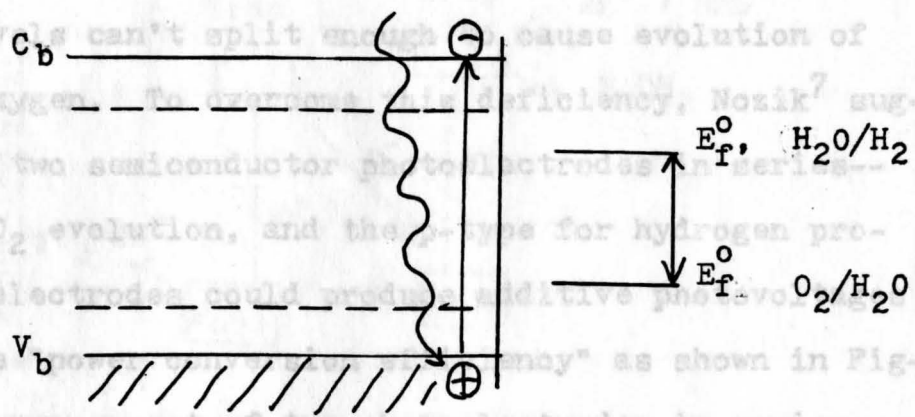


Fig. 11. Diagram of the minimum conditions for the decomposition of water.

Statement of the Problem

Since polymer photoelectrodes would offer more versatility, by addition of light absorbers or other conducting polymers, to harness more useful energy from sunlight, they could conceivably overcome problems inherent in semiconductors. It was desired to construct a monomer of acetylene attached to a polymer (Chrome Azurol S, Figure 14), which when polymerized would mimic a p-type semiconductor. The photoelectrode was used to catalyze the decomposition of water when immersed in an electrolyte.

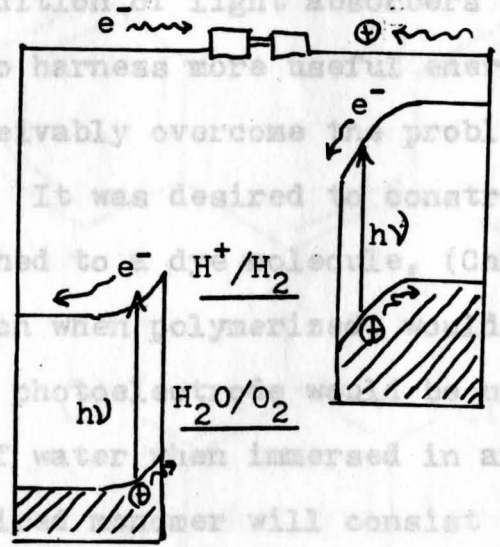


Fig. 12. An n-p photoassisted system.

The design of the polymer will consist of a propargyl group, $(CH_2C\equiv CH_2-)$, and the dye moiety (Chrome Azurol S). The route of synthesis of the polymer was via a Williamson ether synthesis (Figure 15). It entailed a substitution reaction whereby a halogen is substituted by a phenoxide of the

Most semiconductors have too large a band gap to absorb visible light, or are unable to decompose water because Fermi levels can't split enough to cause evolution of hydrogen and oxygen. To overcome this deficiency, Nozik⁷ suggested placing two semiconductor photoelectrodes in series-- an n-type for O₂ evolution, and the p-type for hydrogen production. The electrodes could produce additive photovoltages to increase the "power conversion efficiency" as shown in Figure 12. This arrangement of two photoelectrodes in series mimics the natural arrangement of Photosystems I and II in chloroplasts (Figure 13).

Statement of the Problem

Since polymer photoelectrodes would offer more versatility, by addition of light absorbers or other conducting polymers, to harness more useful energy from sunlight, they could conceivably overcome the problems inherent in semiconductors. It was desired to construct a monomer of acetylene attached to a dye molecule, (Chrome Azurol S, Figure 14), which when polymerized, would mimic a p-type semiconductor. The photoelectrode would be used to catalyze the decomposition of water when immersed in an electrolyte.

The desired monomer will consist of a propargyl group, (CH≡C-CH₂-), and the dye moiety (Chrome Azurol S). The route of organic synthesis employed the Williamson ether synthesis (Figure 15). It entailed a substitution reaction whereby a halogen is substituted by a phenoxide of the

dye to form the monomer, by a stable ether linkage.⁸

The synthesized polymer, polyacetylene, poly(CH), is to be conductive while the organic dye would branch off the polymer as a pendent group, and be used to create an electrical gradient for separating charge and producing a chemical potential when irradiated.

When a p-type semiconductor is immersed in an electrolyte, the majority current carriers (holes) leave the surface of the semiconductor and enter the solution to

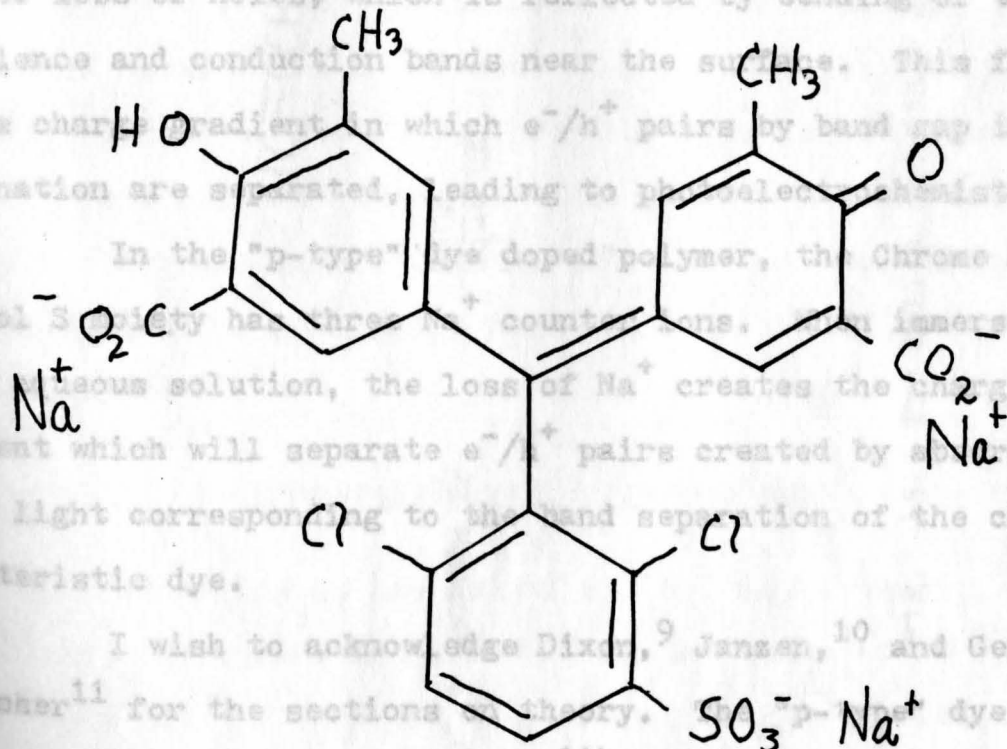
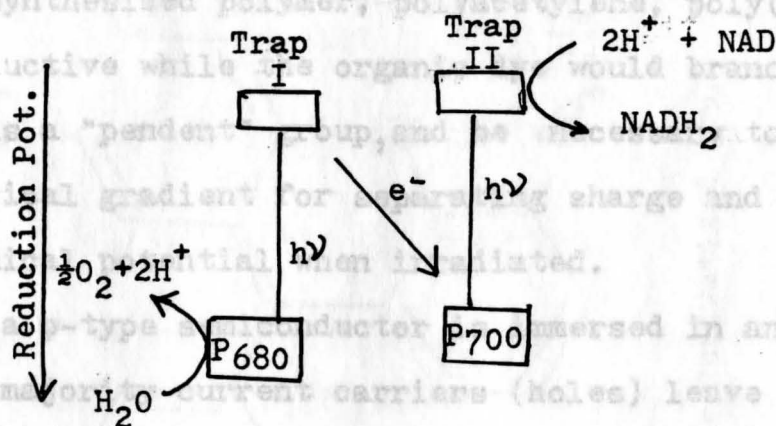
balance the surface of the semiconductor where light is absorbed. The depletion layer will act as a barrier against the further loss of holes, which is reflected by bending of the

valence and conduction bands near the surface. This forms the charge gradient in which e^-/h^+ pairs by band gap illumination are separated, leading to photoelectrochemistry.

In the "p-type" dye-doped polymer, the Chrome Azurol S dye has three counterions. When immersed in an aqueous solution, the loss of Na^+ creates the charge gradient which will separate e^-/h^+ pairs created by absorption of light corresponding to the band separation of the characteristic dye.

I wish to acknowledge Dixon,⁹ Janzen,¹⁰ and Gerlachner¹¹ for the sections of the theory. The p-type dye-doped polymer is due to Mettee.^{11b}

Fig. 14. Structure of Chrome Azurol S.



dye to form the monomer, by a stable ether linkage.⁸

The synthesized polymer, polyacetylene, poly(CH), is to be conductive while the organic dye would branch off the polymer as a "pendent" group, and be necessary to create an electrical gradient for separating charge and producing a chemical potential when irradiated.

When a p-type semiconductor is immersed in an electrolyte, the majority current carriers (holes) leave the surface of the semiconductor and enter the solution to balance the Fermi levels. A depletion layer is created at the surface of the semiconductor where light is absorbed. The depletion layer will act as a barrier against the further loss of holes, which is reflected by bending of the valence and conduction bands near the surface. This forms the charge gradient in which e^-/h^+ pairs by band gap illumination are separated, leading to photoelectrochemistry.

In the "p-type" dye doped polymer, the Chrome Azurol S moiety has three Na^+ counter ions. When immersed in an aqueous solution, the loss of Na^+ creates the charge gradient which will separate e^-/h^+ pairs created by absorption of light corresponding to the band separation of the characteristic dye.

I wish to acknowledge Dixon,⁹ Janzen,¹⁰ and Gerischer¹¹ for the sections on theory. The "p-type" dye doped polymer is due to Mettee.^{11b}

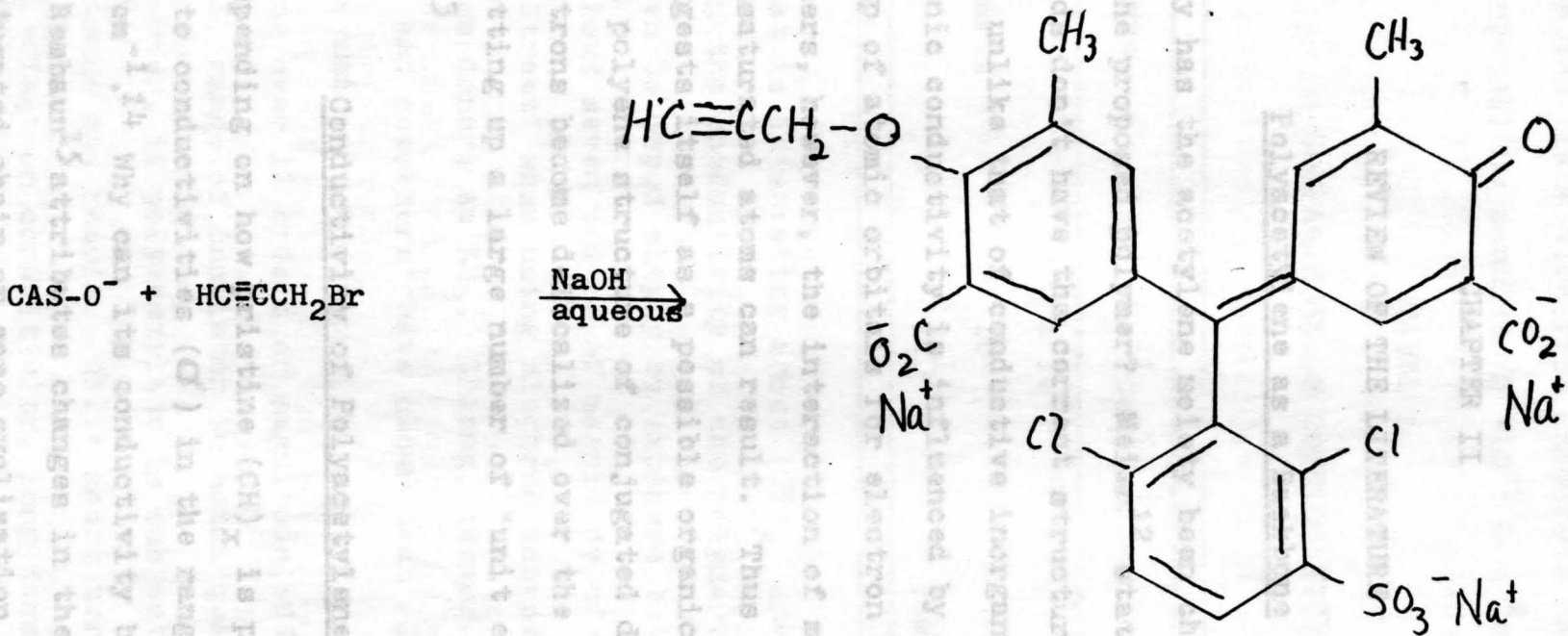


Fig. 15. The Williamson ether synthesis and the derivatized dye.

increase in the transition from amorphous ($\sigma = 10^{-9} - 10^{-12} \text{ ohm}^{-1} \text{ cm}^{-1}$) to crystalline samples ($\sigma = 10^{-5} \text{ ohm}^{-1} \text{ cm}^{-1}$).

CHAPTER II

TABLE 1 REVIEW OF THE LITERATURE

Polyacetylene as a Backbone

Why has the acetylene moiety been chosen as the backbone for the proposed polymer? Meier¹² states that most organic solids don't have the correct structure for electron transport, unlike that of conductive inorganic solids, where by electronic conductivity is influenced by close packing and overlap of atomic orbitals for electron exchange. In some polymers, however, the interaction of molecular orbitals of unsaturated atoms can result. Thus polyacetylene, $(\text{CH})_x$, suggests itself as a possible organic conductor. $(\text{CH})_x$ is a polyene structure of conjugated double bonds. The π electrons become delocalized over the whole structure, thereby setting up a large number of "unit electronic conductors."¹³

Conductivity of Polyacetylene

Depending on how pristine $(\text{CH})_x$ is prepared, it can give rise to conductivities (σ) in the range of 10^{-12} to $10^{-6} \text{ ohm}^{-1} \text{ cm}^{-1}$.¹⁴ Why can its conductivity be varied so greatly? Rembaum¹⁵ attributes changes in the interruptions in the conjugated chain or some cyclization in the $(\text{CH})_x$ chain. Hatano¹⁶ and associates state that conductivity will

increase in the transition from amorphous ($\sigma = 10^{-9} - 10^{-12} \text{ ohm}^{-1} \text{ cm}^{-1}$) to crystalline samples ($\sigma = 10^{-5} \text{ ohm}^{-1} \text{ cm}^{-1}$).

Theory of Conductivity in $(\text{CH})_x$

TABLE 1

The mechanism of conductivity in $(\text{CH})_x$ has been incompletely known. Comparisons of conductivity by Chien²⁰ introduced a unifying concept taken from solid state physics

Structure	σ ($\text{ohm}^{-1} \text{ cm}^{-1}$)	Type
Cu	6×10^5	conductor
Fused quartz	10^{-16}	insulator
CuO	10^{-5}	semiconductor

What is interesting about $(\text{CH})_x$ are the effects doping has on the conductivity of the polymer. Polymer films of $(\text{CH})_x$ can be doped simply by exposure to Br_2 or I_2 for example. About seven orders of magnitude of σ have been observed by Street¹⁷ when using electron acceptors such as BF_3 and electron donors as NH_3 . Chiang, Heeger, MacDiarmid, Shirakawa, and coworkers¹⁸ have shown that $(\text{CH})_x$ can be doped with donors and acceptors to yield n-type and p-type materials ranging over 12 orders of magnitude of σ . This represents a full range of insulator to metal qualities.

However, if polyacetylene is subjected to air, irreversible damage may result. While short term exposure has a positive effect on conductivity, long term exposure to oxygen reduces conductivity irreversibly through peroxide formation and hydroxylation of double bonds.¹⁹

Theory of Conductivity in $(CH)_x$

The mechanism of conductivity in $(CH)_x$ has been incompletely known for many years, and recently Chien²⁰ introduced a unifying concept taken from solid state physics called the "soliton" theory. Chien uses the soliton, a free radical, to interpret the effects of isomerization, doping, and electrical conductivity and uses EPR data as evidence of unpaired spins. Polyacetylene, depending how it is prepared, exists in three isomeric structures. (Figure 16)

When $(CH)_x$ is prepared at -70°C it shows no EPR signal. The predominant structure at this temperature is the cis-transoid configuration. It is inferred that the valence band of the π orbital is filled while the conduction band isn't occupied. As thermal energy is introduced, there is an EPR signal resulting from an isomerization effect between cis and trans portions of $(CH)_x$ as the long and short bonds of the polymer interchange creating the unpaired state.

Chien defines the soliton domain, as where an unpaired spin, or free radical, exists (Figure 17). The domain is formed because there is a change in the phase of the π wave function. The soliton, (S^\cdot) , exists in the center of the domain. This symbol is that of a neutral soliton (charged solitons, S^+ , also exist). It must be noted that the neutral soliton isn't a fixed entity, but can traverse the $(CH)_x$ molecule.



Fig. 17. Defects caused by the soliton domain.



cis-transoid



trans-cisoid



trans-transoid

Fig. 16. Isomeric forms of $(CH)_x$.

These migrations set up what is known as annihilation, where there is interaction between the unpaired spins. (Figure 18) Summary of what Chien's hypothesis says regarding isomerization:

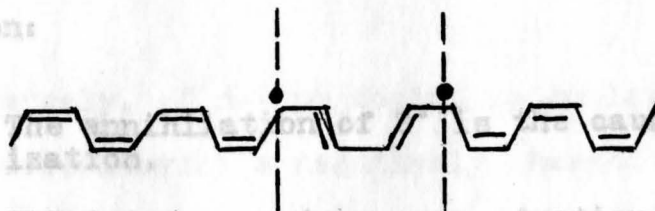


Fig. 17. Defects caused by the soliton domain.

1. The concentration of solitons is a function of isomerization.
2. EPR data suggests a concentration of about one S^{\bullet} per $(CH)_x$.
3. The S^{\bullet} is mobile at room temperature, with its mobility decreasing with temperature. The S^{\bullet} in $(CH)_x$ at $-70^{\circ}C$, (cis form).

Regarding the method of conduction in polyacetylene, it is sure the soliton itself isn't the current carrier. Polyacetylene is a semiconductor, in that the carrier is positively charged. Therefore, the role of the soliton is to cause the formation of h^+ carriers.

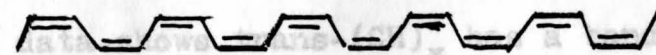


Fig. 18. Migration of solitons and their annihilation.

Experimental data shows a band gap of 1.5 eV, and it is postulated by Chien that solitons are nonbonding electrons and exist somewhere within this band gap. Therefore, it is possible to create holes when electrons leave the lower lying valence band to populate the higher soliton level.

P-type and n-type dopants have also been handled with the soliton theory. In the first case, p-type dopants, the dopant oxidizes S^{\bullet} and converts it to a delocalized carbonium ion. The paramagnetic S^{\bullet} is converted to a spinless soliton, (S^+). Also, it was postulated that the polymer chain could be oxidized, giving rise to a cation radical. The π kink is still maintained in this structure as Fig-

These migrations set up what is known as annihilation, where there is interaction between the unpaired spins. (Figure 18)

Summarizing what Chien's hypothesis says regarding isomerization:

1. The annihilation of S^{\cdot} is the cause of isomerization.

2. EPR data suggests a concentration of about one S^{\cdot} per $(CH)_x$.

3. The S^{\cdot} 's are mobile at room temperature, with its mobility decreasing with temperature. The S^{\cdot} in $(CH)_x$ at $-70^{\circ}C$, (cis form):

Regarding the method of conduction in polyacetylene, it is sure the soliton itself isn't the current carrier. Polyacetylene is a p-type semiconductor at room temperature, in that the carrier is positively charged. Therefore, the role of the soliton is to cause the formation of h^+ carriers.²¹

Experimental data shows trans- $(CH)_x$ has a band gap of 1.5 eV, and it is postulated by Chien that solitons are nonbonding electrons and exist somewhere within this band gap. Therefore, it is possible to create holes when electrons leave the lower lying valence band to populate the higher soliton level.

P-type and n-type dopants have also been handled with the soliton theory. In the first case, p-type dopants, the dopant oxidizes S^{\cdot} and converts it to a delocalized carbenium ion. The paramagnetic S^{\cdot} is converted to a spinless soliton, (S^+) . Also, it was postulated that the poly-chain could be oxidized, giving rise to a cation radical.

The π kink is still maintained in this structure as Fig-

ure 19 shows. Both of these processes occur simultaneously, and depend on the types of acceptors used. The changes are viewed with EPR as increase, decrease, or no net change in the EPR.

Conversely, if n-type doping is employed, reduction of the S^+ occurs leaving a negatively charged soliton, (S^-). If reduction takes place on the polymer chain a radical anion is formed (Figure 20).

Chien's last statement pertains to conduction. He notes that conduction of doped $(CH)_x$ is the result of carrier rather than charge transfer. These results were concluded from work done with conductivity and thermopower, (ρ), in doped $(CH)_x$.

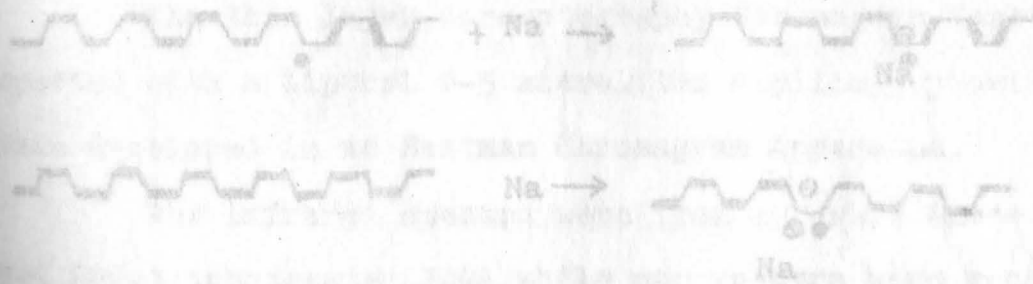


Fig. 20. (Top); Reduction occurs at the S^+ forming a delocalized carbanion. (Bottom); Reduction elsewhere in the polymer forming a radical anion. (where \equiv = C=C and $-$ = C-C)

CHAPTER III

EXPERIMENTAL

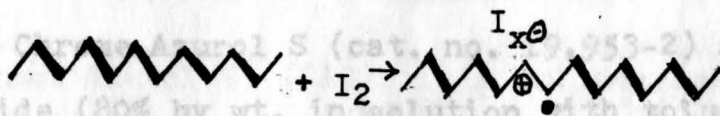
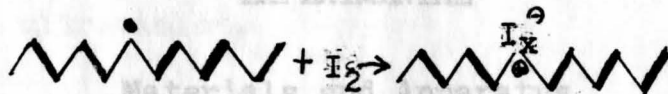


Fig. 19. (Top), The dopant oxidizes S[•] directly forming a carbenium ion. (Bottom), The dopant oxidizes the polymer chain directly forming a cation radical. (where \equiv = C=C and $-$ = C-C)

oxide (99.8% atom D) came from Aldrich also. Potassium bromide and sodium sulfate were analytical grade Baker Analyzed Reagents. Chloroform and acetic acid were from Fisher Scientific. Ethanol and n-butanol came from Mallinckrodt. All water was either distilled or deionized.

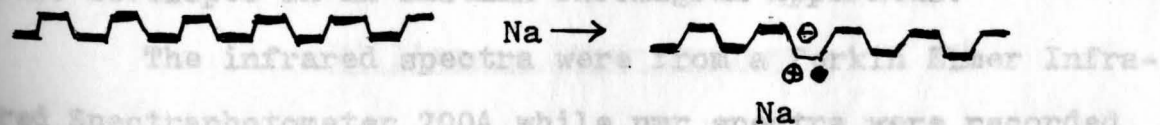
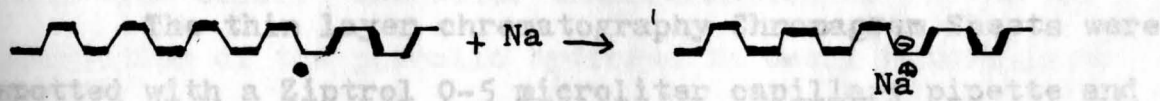


Fig. 20. (Top), Reduction occurs at the S[•] forming a delocalized carbanion. (Bottom), Reduction elsewhere in the polymer forming a radical anion. (where \equiv = C=C and $-$ = C-C)

Applied (Model 1024) x-y Recorder, and a Sabtronics (Model 8033) Multimeter to follow the potential. The Navetec (Model 142) HP VCG Generator was employed for the sawtooth wave needed in cyclic voltammetry.

The illumination source was a 300W mercury-xenon arc lamp, by Hanovia Lab.

CHAPTER III

Filtered by 10 cm of water to remove the infrared. The radiation consisted of visible and ultraviolet.

EXPERIMENTAL

Materials and Apparatus

The Chrome Azurol S (cat. no. 19,953-2) and propargyl bromide (80% by wt. in solution with toluene for stabilization; cat. no. P5,100-1) was purchased from the Aldrich Chemical Company, Milwaukee, Wisconsin. Deuterium oxide (99.8% atom D) came from Aldrich also. Potassium bromide and sodium sulfate were analytical grade Baker Analyzed Reagents. Chloroform and acetic acid were from Fisher Scientific. Ethanol and n-butanol came from Mallinckrodt. All water was either distilled or deionized.

The thin layer chromatography Chromagram Sheets were spotted with a Ziptrol 0-5 microliter capillary pipette and were developed in an Eastman Chromagram Apparatus.

The infrared spectra were from a Perkin Elmer Infra-red Spectrophotometer 700A, while nmr spectra were recorded on a Varian Anaspect EM-360 (60 MHz).

Cyclic voltammetry required an EG&G Princeton Applied Research (Model 364) Polarographic Analyzer, a Valtec (Model 1024) x-y Recorder, and a Sabtronics (Model 2010A) Multimeter to follow the potential. The Wavetek (Model 142) HP VCG Generator was employed for the sawtooth wave needed in cyclic voltammetry.

The illumination source was a 1000W mercury-xenon arc lamp, by Hanovia Lamp Division, filtered by 10 cm of water to remove the infrared. The radiation consisted of visible and ultraviolet.

Chemistry of Chrome Azurol S

Chrome Azurol S, (CAS), is a triphenylmethane type dye derivative that is quite soluble in water. Its ionic character is contributed by three acidic functions, in addition to the phenolic hydrogen. Two of the acidic functions are carboxylate while the third is a sulfonate group (Figure 14).

One important property of this dye was its pH/color dependence. In acidic and neutral aqueous solutions, the dye has a deep red color. In basic solutions, CAS takes on a deep blue color. The color transformation is due to the ionization of the phenolic hydrogen in basic solution, as shown in Figure 21.

Williamson Ether Synthesis

CAS (2g) was added to an aqueous solution (50 ml) of sodium hydroxide (0.3g) in a three necked round bottom flask. Propargyl bromide (1 ml) was added to the aqueous solution and refluxed for 2 hours (Figure 22). The reaction mixture was kept below 80°C so the propargyl bromide wouldn't polymerize. Initially, the solution was a deep blue color, indicative of the phenoxide ion present. During the refluxing, the pH was monitored periodically so that conditions

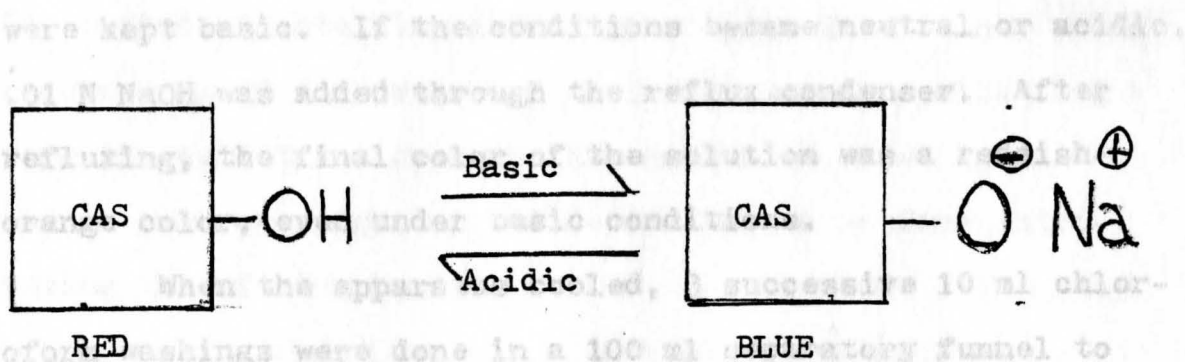


Fig. 21. The color transformation of CAS is due to the phenolic hydrogen. In basic conditions, the hydrogen is lost and the phenoxide is formed. Acidity provides attachment of the hydrogen back onto CAS.

Thin Layer Chromatography

TLC was performed to show that the CAS starting material could be separated from propargyl-coupled monomer, since they have such closely related structures. A TLC Eastman Chromagram sheet of silica gel G, was spotted with a 5 microliter sample of the and the monomer. The samples were developed for hours. The solvent system employed a 60:20:10:10 of ethyl acetate, ethanol, and water, as described by [reference].

Fig. 22. The apparatus for the Williamson Ether Synthesis.

The IR background of pure KBr is limited to a few easily identified bands, which was the reason for choice.

were kept basic. If the conditions became neutral or acidic, .01 N NaOH was added through the reflux condenser. After refluxing, the final color of the solution was a reddish-orange color, even under basic conditions. When the apparatus cooled, 3 successive 10 ml chloroform washings were done in a 100 ml separatory funnel to remove the unreacted propargyl bromide. The aqueous layer was transferred to a Büchner funnel and suction filtered to remove any residue. The product, in aqueous solution, was flash evaporated with a cold trap/ vacuum pump system at 5-10 torr. The final product was an orange powder. It was quite different in color from the red crystals of CAS.

Thin Layer Chromatography

TLC was performed to show that the CAS starting material could be separated from the propargyl-coupled monomer, since they have such closely related structures. A TLC Eastman Chromagram sheet, of silica gel G, was spotted with a 5 microliter sample of the CAS and the monomer. The samples were developed for 2 hours, during which time the samples travelled 4.5 to 5.5 cm. The solvent system employed a 60:20:10:10 of n-butanol, acetic acid, ethanol, and water, as described by Venkataraman.²²

Infrared Data

The ir background of pure KBr is limited to a few easily identified bands, which was the reason for choice.

The method of obtaining a KBr pellet came from Stine.²³ It required a 30 ton press and a die to cast the pellet. Before the pellet was cast the KBr had to be dried in a vacuum oven overnight at 110°C, to keep water from introducing interfering bands.

Nuclear Magnetic Resonance

Since CAS and the monomer were soluble, deuterium oxide was chosen as the solvent. TMS was used as an external standard because of its insolubility in water.

Cyclic Voltammetry

Cyclic voltammetry (CV) was employed as a method to electropolymerize the monomer. Generally, CV can be used to detect any chemical species that is electroactive, i.e., that can undergo redox chemistry. In this technique, the potential of the working electrode is the controlled parameter, which causes a chemical species near the electrode to be oxidized or reduced.

The potential can be interpreted as an "electron pressure" which forces a species into solution to gain e^- (reduction) or lose e^- (oxidation). As the potential of the electrode becomes more negative, it becomes more strongly reducing. Likewise, the more positive the electrode becomes, the more oxidizing it is.

The current (i) is a measure of the amount of electron flow. When a reaction occurs at the electrode, this

current is proportional to the concentration of the electroactive species near the electrode. A cathodic current is usually assigned a positive sign, and that due to oxidation a negative value. If the electrode potential is swept from negative to positive, and a negative current is noted, the current is referred to as an "anodic wave," (Figure 23).

The CV cell was a triple compartment, Pyrex H-type cell whose sections were separated by glass frits. Quartz windows were placed on two of the compartments for photochemical work. The platinum electrode was the working electrode, while the counter electrode was silver. The third, a reference electrode, (SCE), was used to refer the working electrode voltage to.

Aqueous $.1 \text{ N Na}_2\text{SO}_4$ was employed as the electrolyte, whose usable window was measured between $-.58\text{V}$ to $+1.14\text{V}$. Outside these limits, water will either be oxidized or reduced.

Electrolyte solutions of CAS, propargyl bromide, and the monomer were measured first to determine if any differences in their voltammograms existed. Different scan rates were used for the voltammograms of the monomer solution to determine if currents were a surface attached or a dissolved species. A fixed voltage experiment was run at 1.15V for 2 hours, to form a film, and then subjected to CV. Finally, the 1000W power supply was employed to measure any photoelectrochemical effects.

CHAPTER IV

RESULTS AND DISCUSSION

Monomer Evidence

Williamson Ether Synthesis

The color changes of the solution in the Williamson synthesis were helpful. The initial deep blue solution indicated the phenoxide needed for the coupling reaction was present. Subsequently, the solution became a reddish-orange, like the protonated CAS, indicating the coupling of a nonconjugated group to phenoxide.

Except for the ether linked acetyl group, the only other mode of attachment would have been an ester linkage between the propargyl group and one of the acidic functions. Morrison and Boyd note that acidic conditions are required for this esterification, and furthermore, hydrolysis of an ester often occurs under warm acidic or basic conditions.

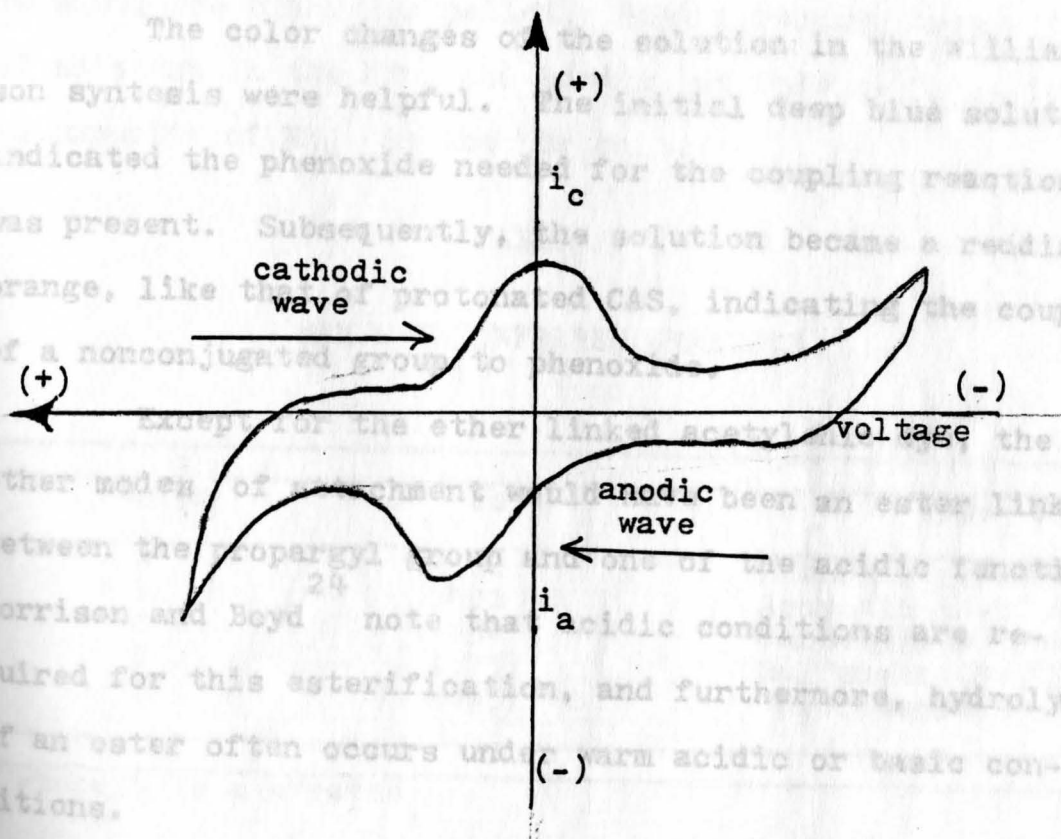


Fig. 23. A cyclic voltammogram illustrating the positions of the cathodic wave (swept left to right), and the anodic wave (swept right to left).

Alteration between CAS and the derivatized dye is that an ether linkage would have replaced the phenolic hydrogen in CAS. Qualitative TLC plates showed that a compound in addition to CAS was present. A new yellow pigment, presumed to be the derivatized monomer, was spotted above

the CAS red pigment on the silica layer.

CHAPTER IV

RESULTS AND DISCUSSION

Monomer Evidence

Williamson Ether Synthesis

The color changes of the solution in the Williamson synthesis were helpful. The initial deep blue solution indicated the phenoxide needed for the coupling reaction was present. Subsequently, the solution became a reddish-orange, like that of protonated CAS, indicating the coupling of a nonconjugated group to phenoxide.

Except for the ether linked acetylenic dye, the only other modes of attachment would have been an ester linkage between the propargyl group and one of the acidic functions. Morrison and Boyd²⁴ note that acidic conditions are required for this esterification, and furthermore, hydrolysis of an ester often occurs under warm acidic or basic conditions.

Thin Layer Chromatography

The only alteration between CAS and the derivatized dye is that an ether linkage would have replaced the phenolic hydrogen in CAS. Qualitative TLC plates showed that a compound in addition to CAS was present. A new yellow pigment, presumed to be the derivatized monomer, was spotted above

the CAS red pigment on the silica layer.

Infrared Data

The KBr pellet proved to be essential in identifying the groups of the CAS, but evidence of the acetylenic triple bond could not be established. The use of Silverstein²⁵ was employed in identifying the spectra. Figure 24 shows the blank KBr pellet. Band A results from a trace of moisture in the KBr, and band B, at 1420 cm^{-1} , is from an impurity of NH_4^+ in the KBr salt.

TABLE 2

BANDS IN INFRARED ANALYSIS

Region	cm^{-1}	Type
A	3500	Phenolic (O-H) δ
B	3000	Aromatic (C-H) δ
C	1650	Carboxylate (C=O) δ
D	1175	Sulfonate (S=O) δ
E	1095	Chlorobenzene

where δ is a stretch

The ir spectrum of CAS helped confirm the presence of substituent groups of the carboxylate, sulfonate, and chlorobenzene as shown in Figure 25. The ir of the derivatized CAS didn't reveal the presence of an acetylenic group, however, ($2140\text{-}2190\text{ cm}^{-1}$). The weakness of all the bands in the monomer spectrum may have precluded seeing the (HC \equiv C-) group.

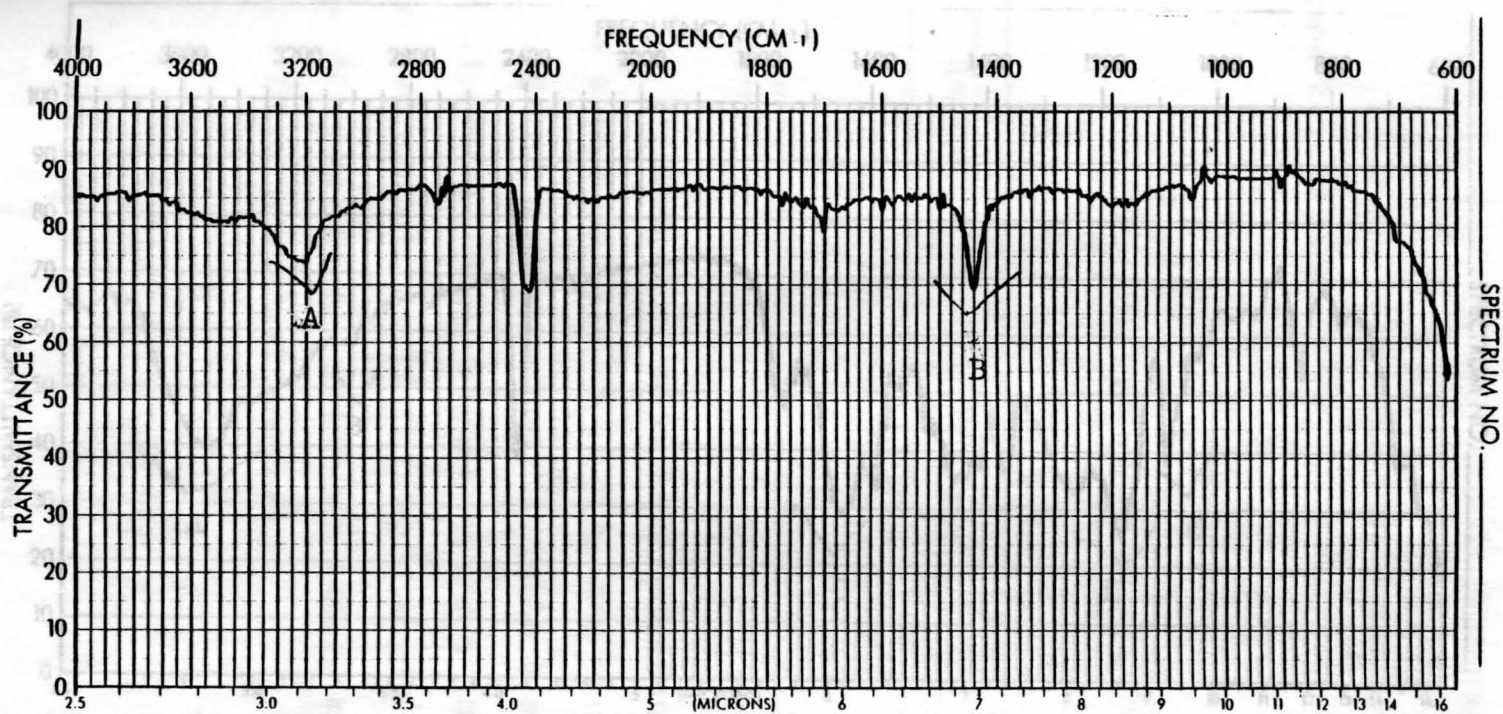


Fig. 24. ir spectrum of KBr pellet, (blank).

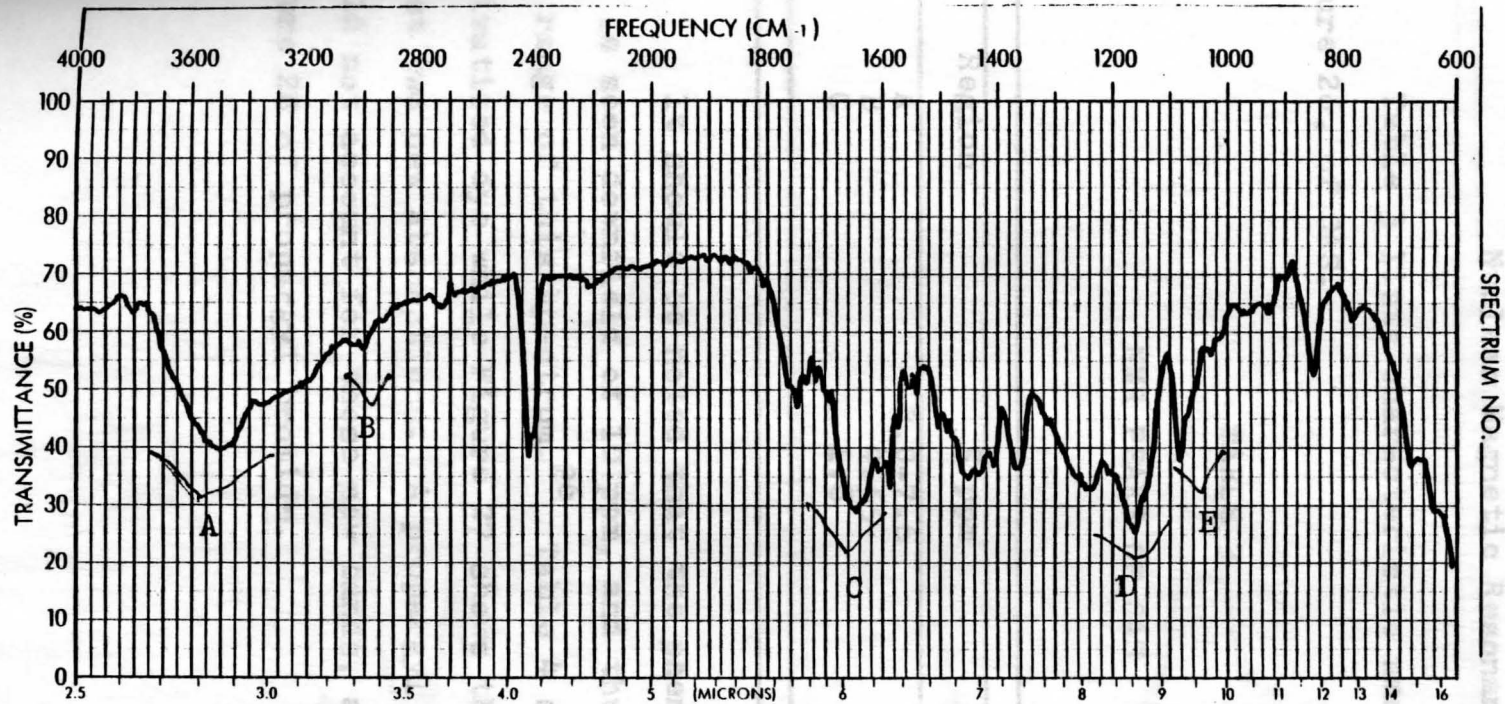


Fig. 25. ir spectrum of CAS.

Nuclear Magnetic Resonance

Table 3 lists characteristic nmr peaks as shown in Figure 26, of CAS.

TABLE 3
NMR PEAKS OF CAS

Region	δ ppm	Type
A	7.0-7.6	Ar H
B	4.55	H ₂ O (impurity)
C	1.8	-CH ₃

It should be noted that the phenolic hydrogen of CAS is seen downfield of 10 ppm, and thus, isn't within the range of this spectrum.²⁶ Table 4 shows the nmr of the derivatized dye while Figure 27 shows the inclusion of at least two new absorptions. A propargyl bromide impurity would not account for these new bands, as can be seen in Figure 28 of propargyl bromide.

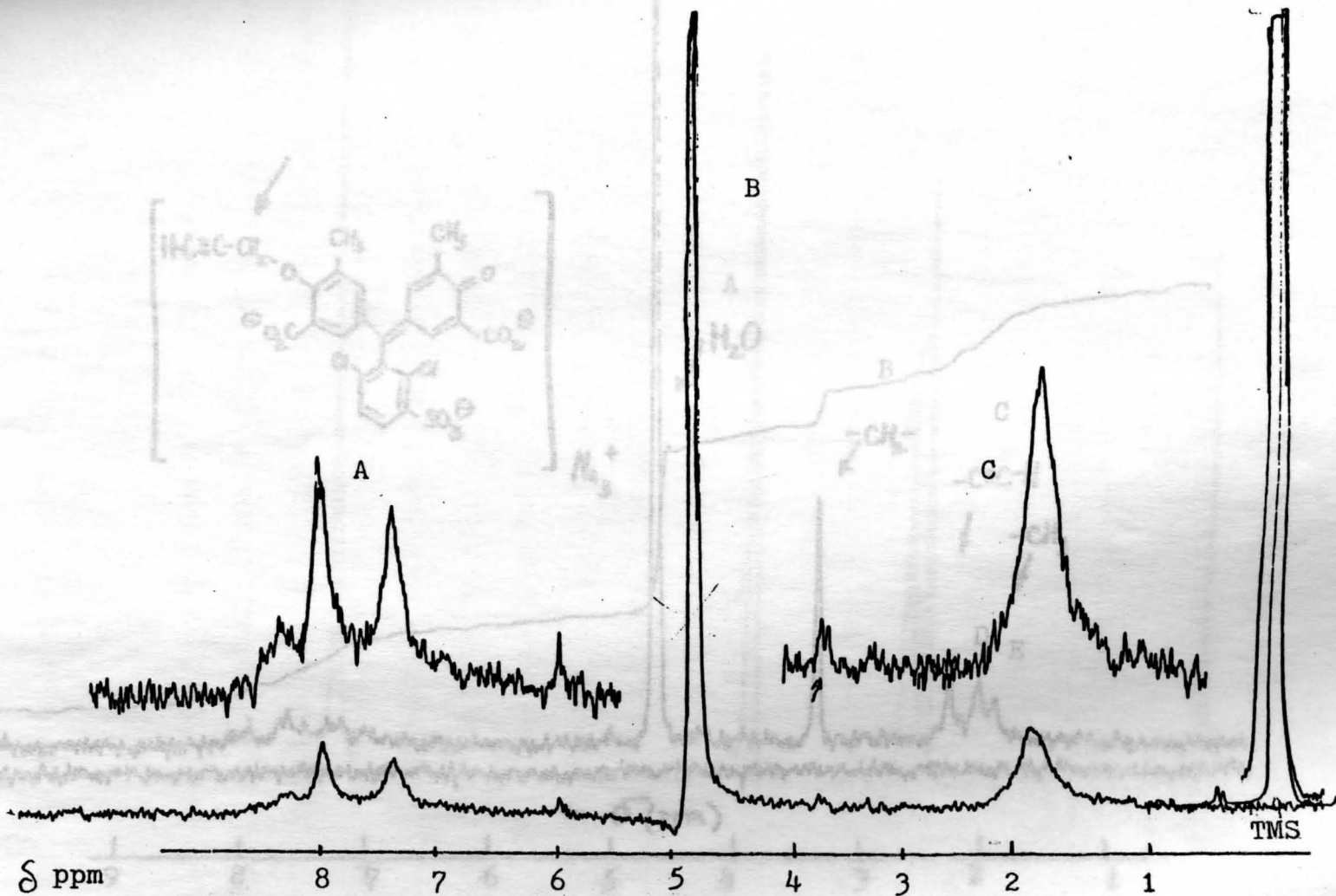


Fig. 26. nmr. spectrum of CAS. (Structure in upper left).

HCOCH_2Br

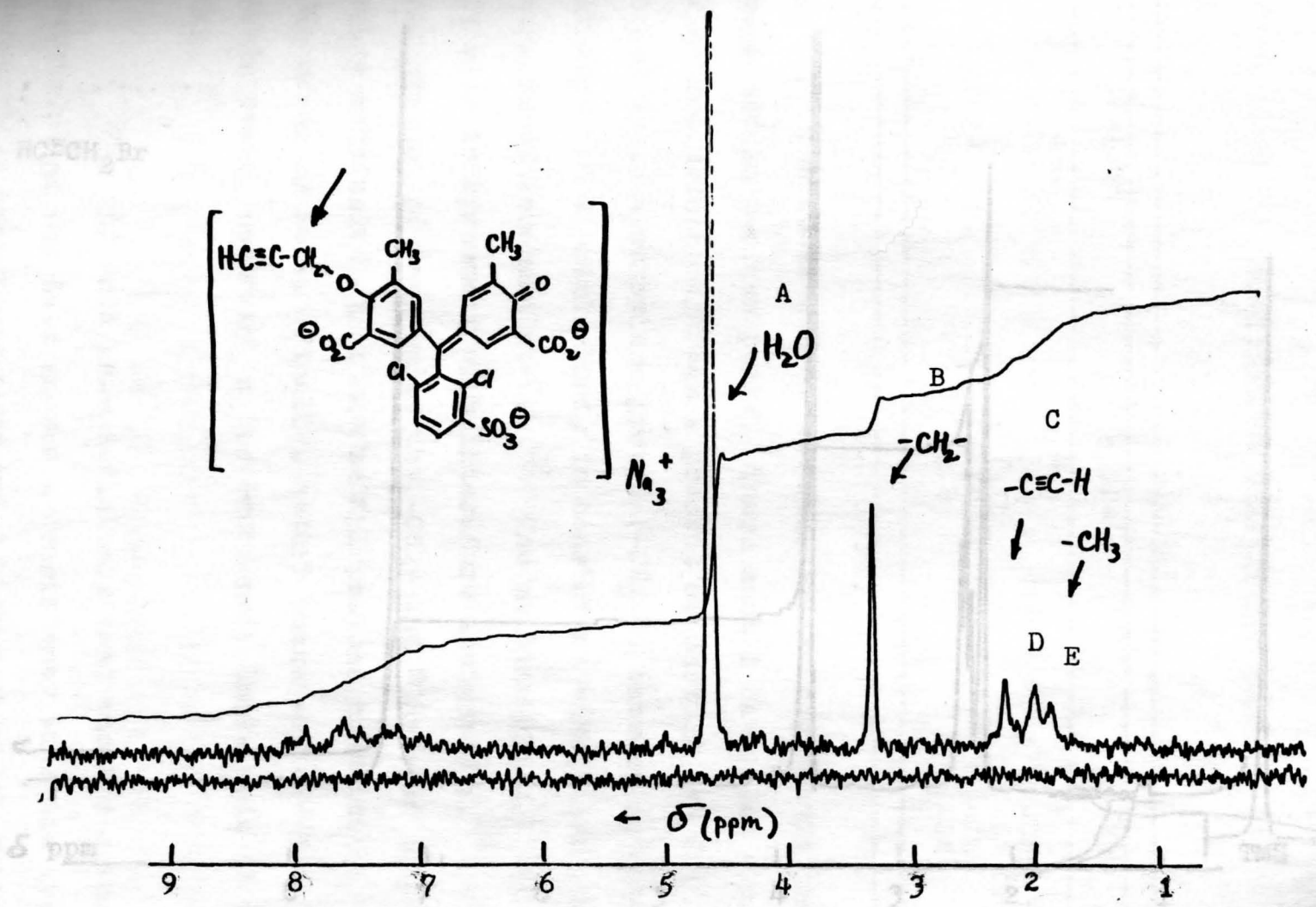
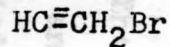


Fig. 27. nmr. spectrum of monomer. (Structure in upper left).

in above left corner)



δ ppm

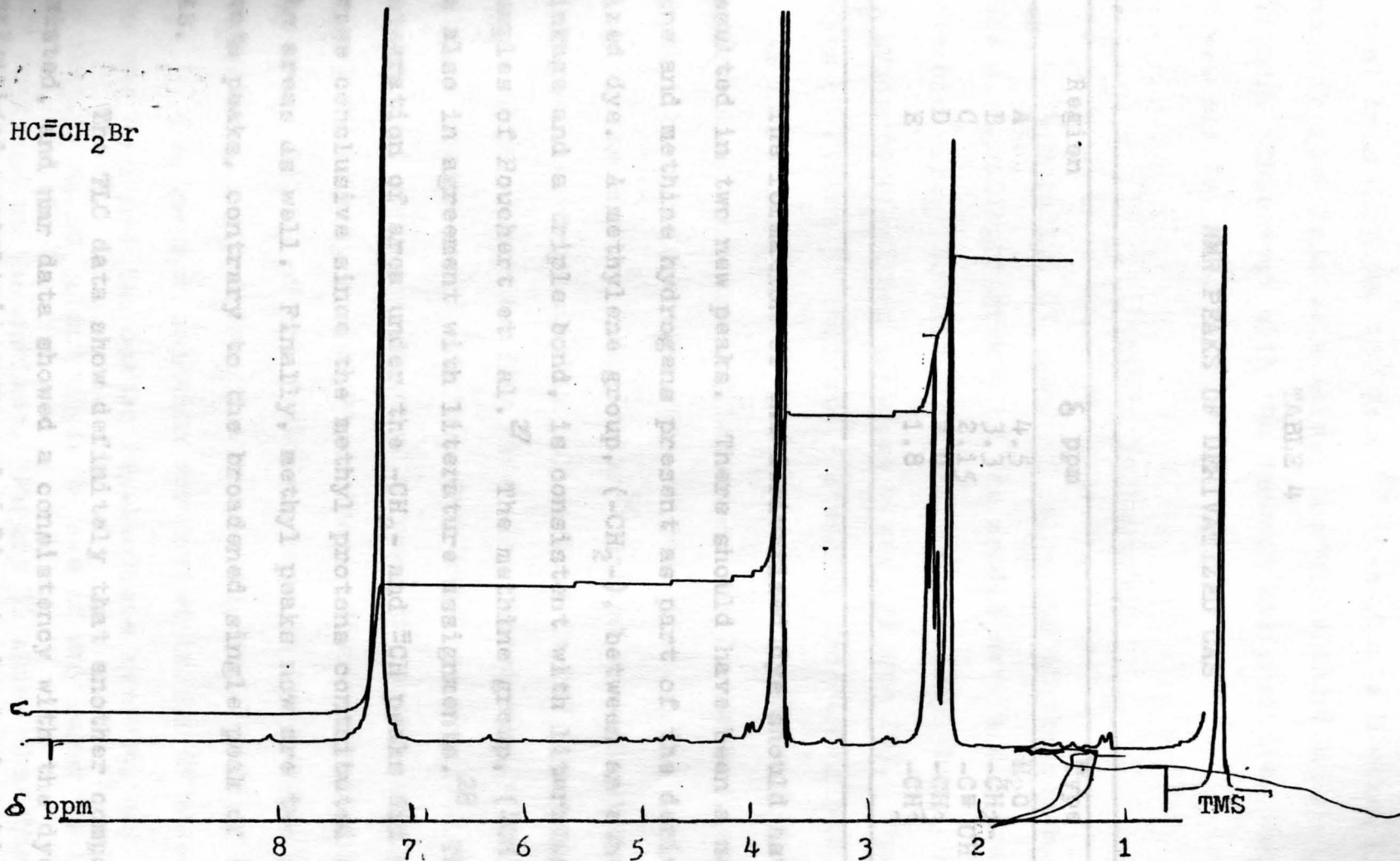


Fig. 28. nmr spectrum of propargyl bromide. (structure is in above left corner)

a test from Morrison and Boyd.²⁹ Acetylenic H atoms are known to give insoluble silver acetylide under acidic conditions. This test with the monomer was positive, whereas

TABLE 4

NMR PEAKS OF DERIVATIZED CAS

Region	δ ppm	Type
A	4.5	H ₂ O
B	3.3	-CH ₂ -
C	2.15	-C \equiv CH
D	2.0	-CH ₃
E	1.8	-CH ₃

The formation of the derivatized dye should have resulted in two new peaks. There should have been a methylene and methine hydrogens present as part of the derivatized dye. A methylene group, (-CH₂-), between an ether linkage and a triple bond, is consistent with literature samples of Pouchert et al.²⁷ The methine group, (\equiv CH), is also in agreement with literature assignments.²⁸ The integration of area under the -CH₂- and \equiv CH peaks did not prove conclusive since the methyl protons contributed to the areas as well. Finally, methyl peaks now are two separate peaks, contrary to the broadened single peak of the CAS. The monomer solution was cycled in the CV apparatus

for one hour and the coated Pt electrode removed, and immersed in the 0.1M Na₂SO₄ electrolyte to see if any layer (polymer) existed, and nmr data showed a consistency with the dye was retained on the surface. Figure 31 shows that the derivatized acetylenic compound. Direct chemical evidence of a triple bond in the derivatized CAS was obtained using

a test from Morrison and Boyd.²⁹ Acetylenic H atoms are known to give insoluble silver acetylides under acidic conditions. This test with the monomer was positive, whereas it was not for CAS.

Cyclic Voltammetry

Generally, CV scans of solutions of the monomer show a significant growth of the anodic wave and a decreasing cathodic wave. Solutions of CAS and propargyl bromide show no evidence of either of these waves (Figure 29). The results of Figure 30 indicate a steadily increasing conductivity in the oxidation region, which is consistent with a progressive deposition of layers on the Pt surface, which in turn become less conducive to reduction.

The work of Subramanian³⁰ showed that phenylacetylene could be electrochemically polymerized in DMF, so that a layer of polyacetylene may have also formed on the electrode in this thesis work. On the other hand, the layer could be a series of monomers attached through the acetylenic linkages individually to the Pt surface. Steric considerations, and the lability of the ($-C\equiv CH$) groups to free radical polymerization, suggest that the former is more likely.

The monomer solution was cycled in the CV apparatus for one hour and the coated Pt electrode removed, and immersed in the $.1N Na_2SO_4$ electrolyte to see if any layer (polymer) was retained on the surface. Figure 31 shows that the anodic wave didn't reappear, but it seems that the cathodic

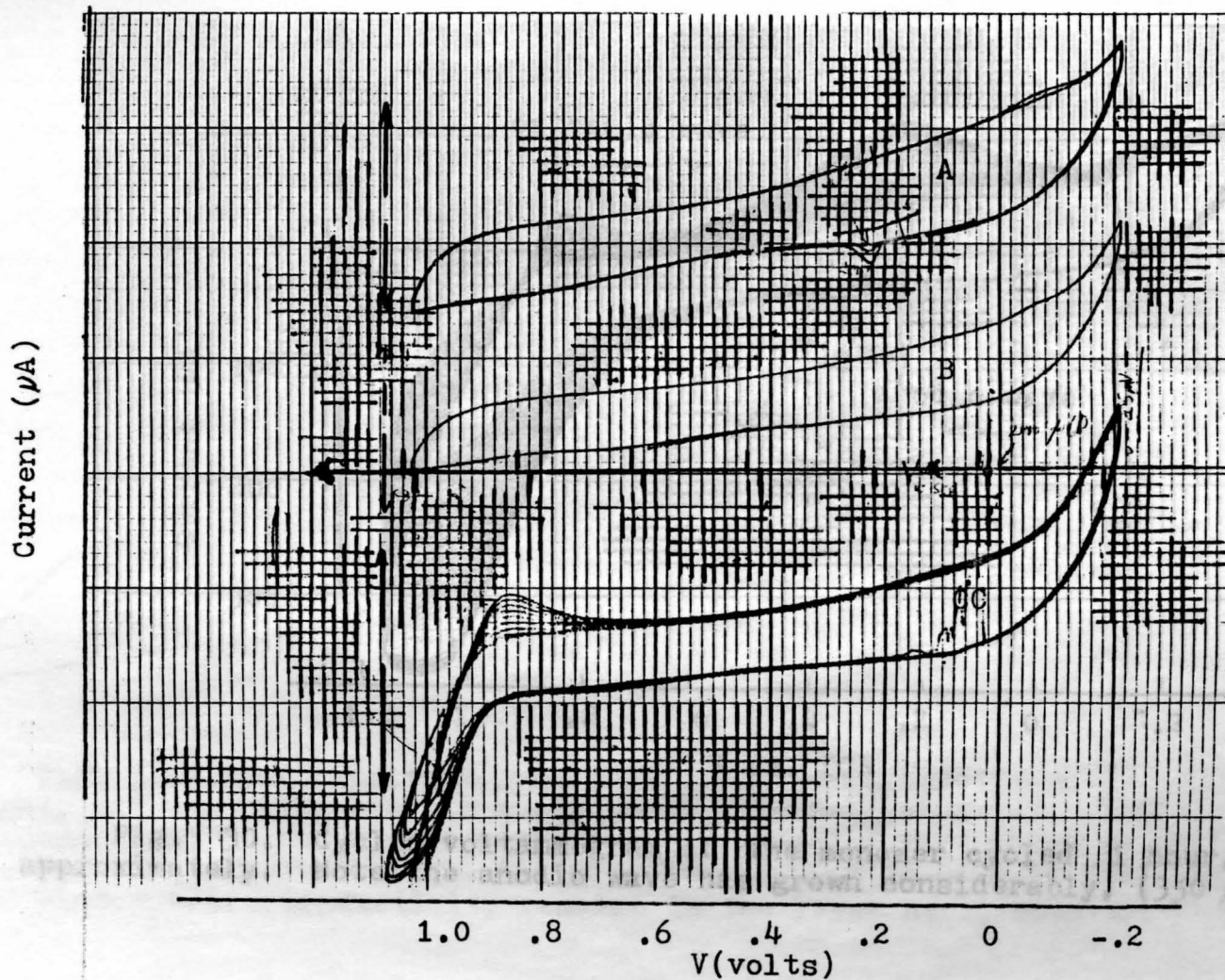


Fig. 29. Cyclic voltammogram of: (A) CAS, (B) $.1N$ Na_2SO_4 , and (C) the monomer, (CAS-O- $CH_2C\equiv CH$): amplitudes increase each sweep.

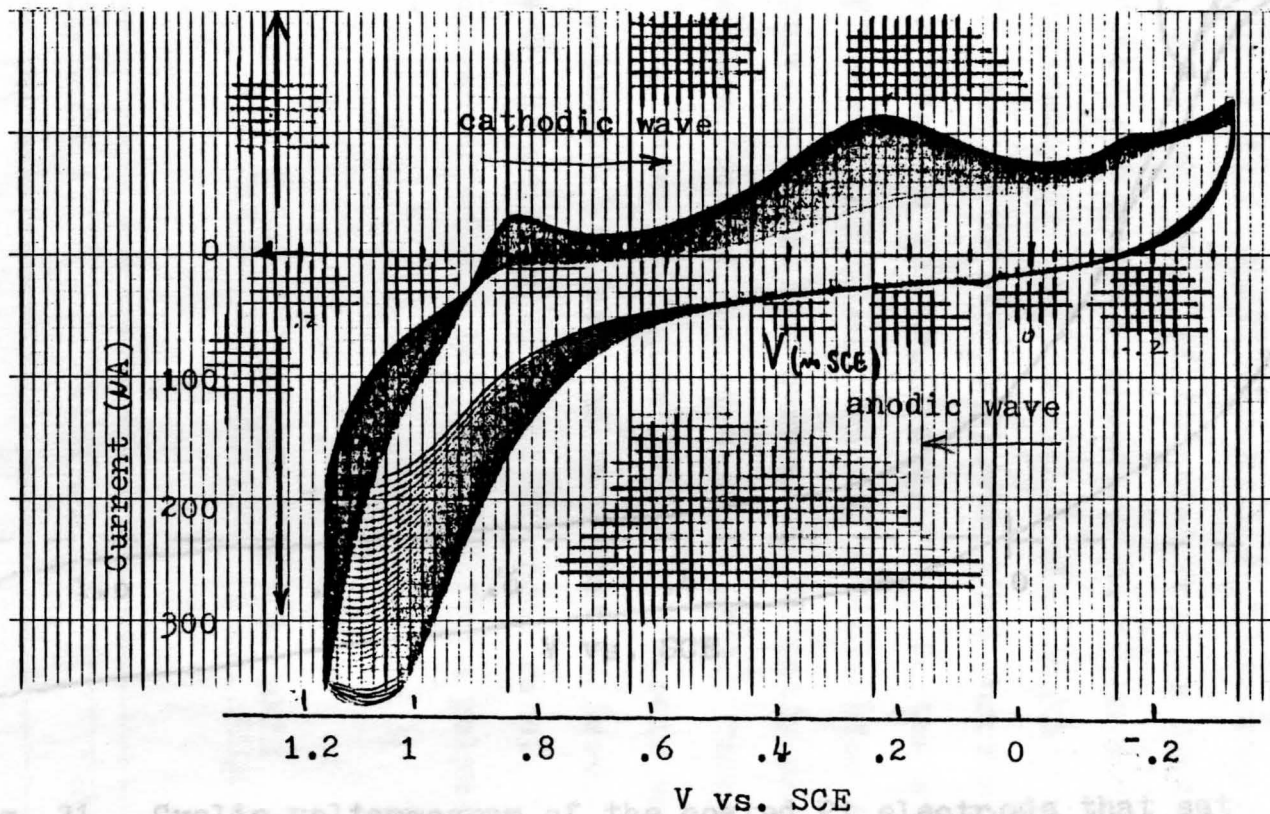


Fig. 30. Cyclic voltammogram of the monomer cycled 1 hour, approximately. Note the anodic wave has grown considerably, (350 μ A).

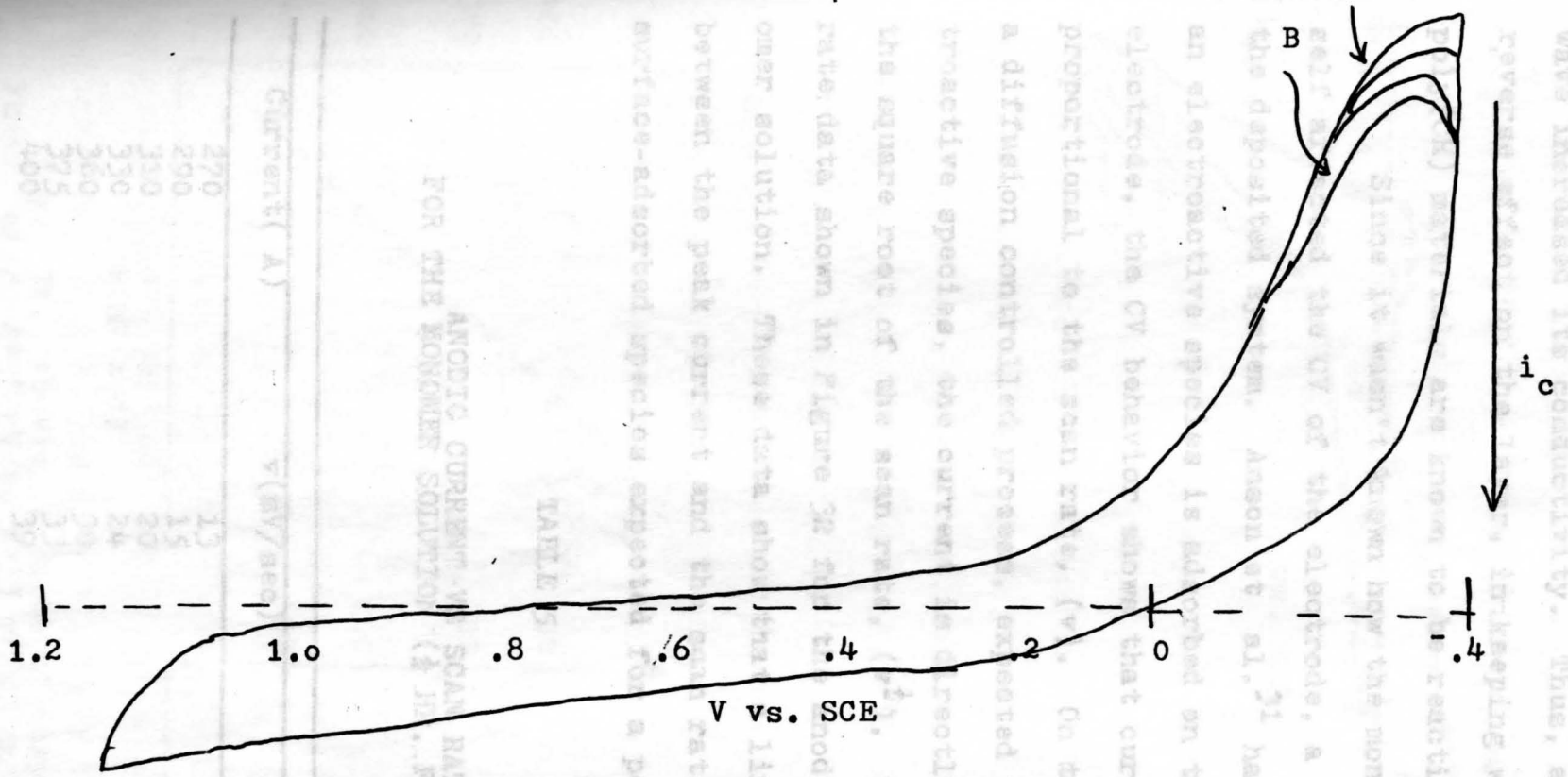


Fig. 31. Cyclic voltammogram of the coated Pt electrode that sat overnight, and was reimmersed in a .1N Na_2SO_4 the following day. There is no enhancement of the anodic wave, but the cathodic wave shows an initially increase in the cathodic current (A) and then it reverts back to the electrolyte window (B). Conductivity remains in the layer here, however.

wave increased its conductivity. Thus, air exposure had a reverse effect on the layer, in keeping with the fact that poly(CH) materials are known to be reactive with air.

Since it wasn't known how the monomer solution itself affected the CV of the electrode, a study was done on the deposited system. Anson et al.³¹ have shown that if an electroactive species is adsorbed on the surface of an electrode, the CV behavior shows that current is directly proportional to the scan rate, (v). On the other hand, for a diffusion controlled process, expected for dissolved electroactive species, the current is directly proportional to the square root of the scan rate, ($v^{\frac{1}{2}}$). Table 5 lists scan rate data shown in Figure 32 for the anodic wave in monomer solution. These data show that a linearity exists between the peak current and the scan rate, indicating a surface-adsorbed species expected for a polymer layer.

TABLE 5
ANODIC CURRENT VS SCAN RATE
FOR THE MONOMER SOLUTION ($\frac{1}{2}$ HR. FILM GROWTH)

Current (A)	v (mV/sec)	$v^{\frac{1}{2}}$ (mV/sec) ^{$\frac{1}{2}$}
270	13	3.6
290	15	3.9
310	20	4.5
330	24	4.9
360	30	5.5
375	33	5.7
400	39	6.2

Fig. 32. Above: Results of varying the scan rate, where $A=33$ mV/s, $B=33$ mV/s, and $C=39$ mV/s.

the electroactive species on the surface of the electrode.

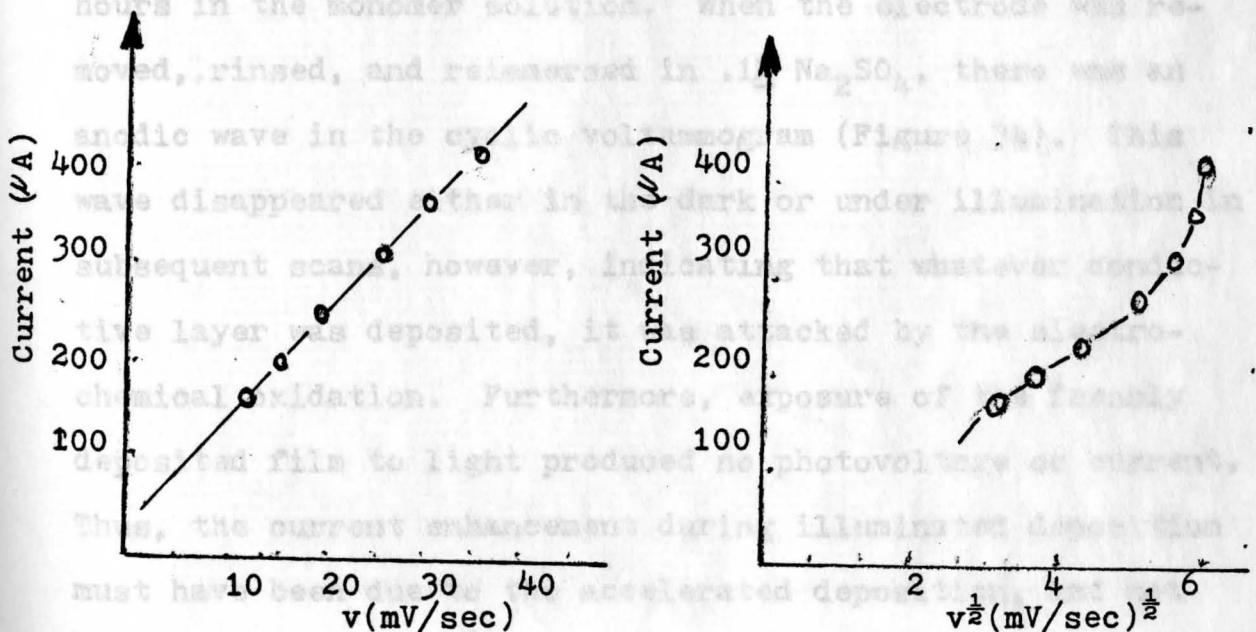
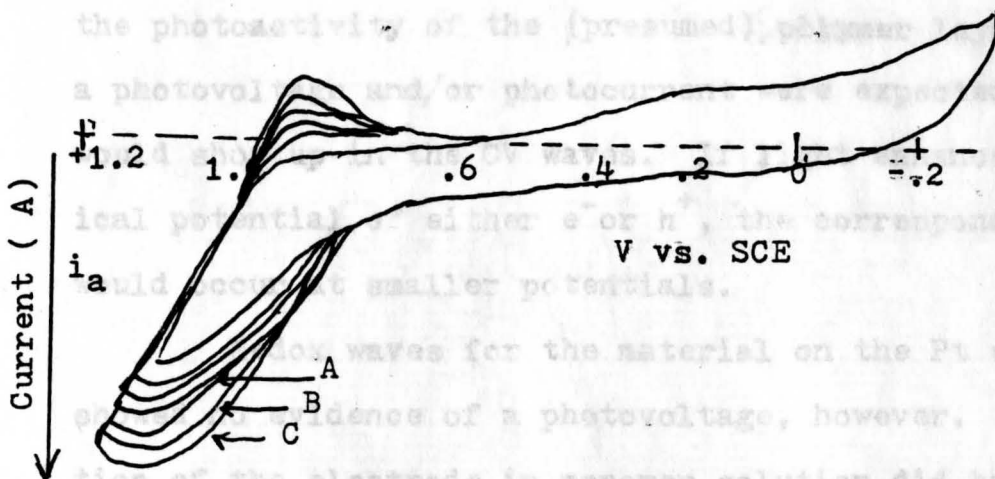


Fig. 32. Above: results of varying the scan rates, where A=33 mV/s, B=33 mV/s, and C=39 mV/s. Below: results of plotting i_a vs. v and i_a vs. $v^{1/2}$. There is linearity on the left indicating adsorption of the electroactive species on the surface of the electrode.

A 1000W lamp, (UV and visible), was used to measure the photoactivity of the (presumed) polymer layer. Either a photovoltage and/or photocurrent were expected, which would show up in the CV waves. If light enhanced the chemical potential of either e^- or h^+ , the corresponding waves would occur at smaller potentials.

Redox waves for the material on the Pt electrode showed no evidence of a photovoltage, however. Illumination of the electrode in monomer solution did have an effect on the current (Figure 33). There appeared to be either an acceleration of the deposition of the conductive layer, or an increased conductivity in the layer itself.

Lastly, the potential of the coated electrode was poised at +1.15V, where the anodic wave occurred, for two hours in the monomer solution. When the electrode was removed, rinsed, and reimmersed in .1M Na_2SO_4 , there was an anodic wave in the cyclic voltammogram (Figure 34). This wave disappeared either in the dark or under illumination in subsequent scans, however, indicating that whatever conductive layer was deposited, it was attacked by the electrochemical oxidation. Furthermore, exposure of the freshly deposited film to light produced no photovoltage or current. Thus, the current enhancement during illuminated deposition must have been due to the accelerated deposition, and not the creation of e^-/h^+ pairs in the layer itself.

The results of CV suggest there is adsorption onto the electrode surface of some partially conductive layer,

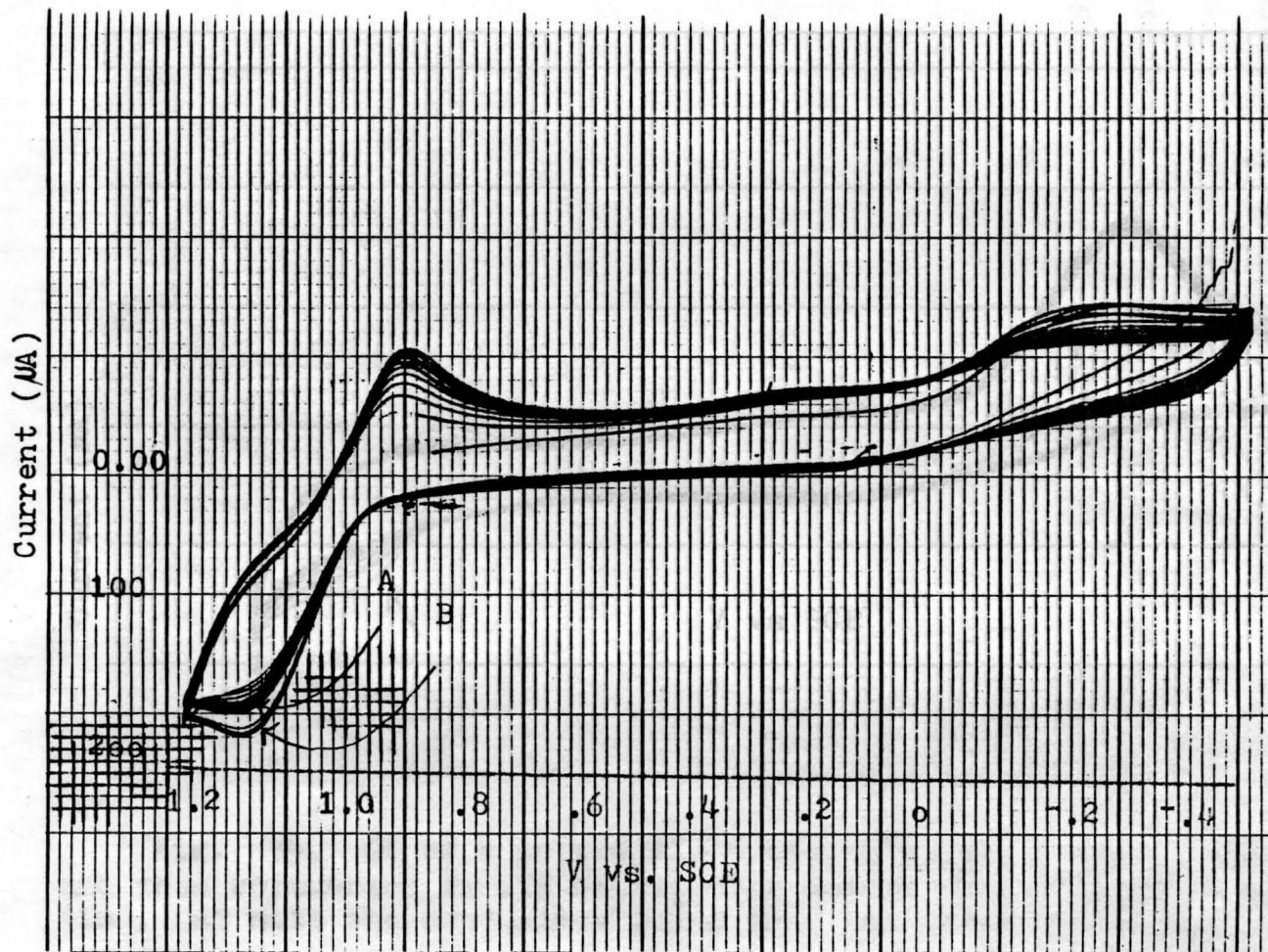


Fig. 33. CV of monomer solution in (A) Dark, (B) Illuminated

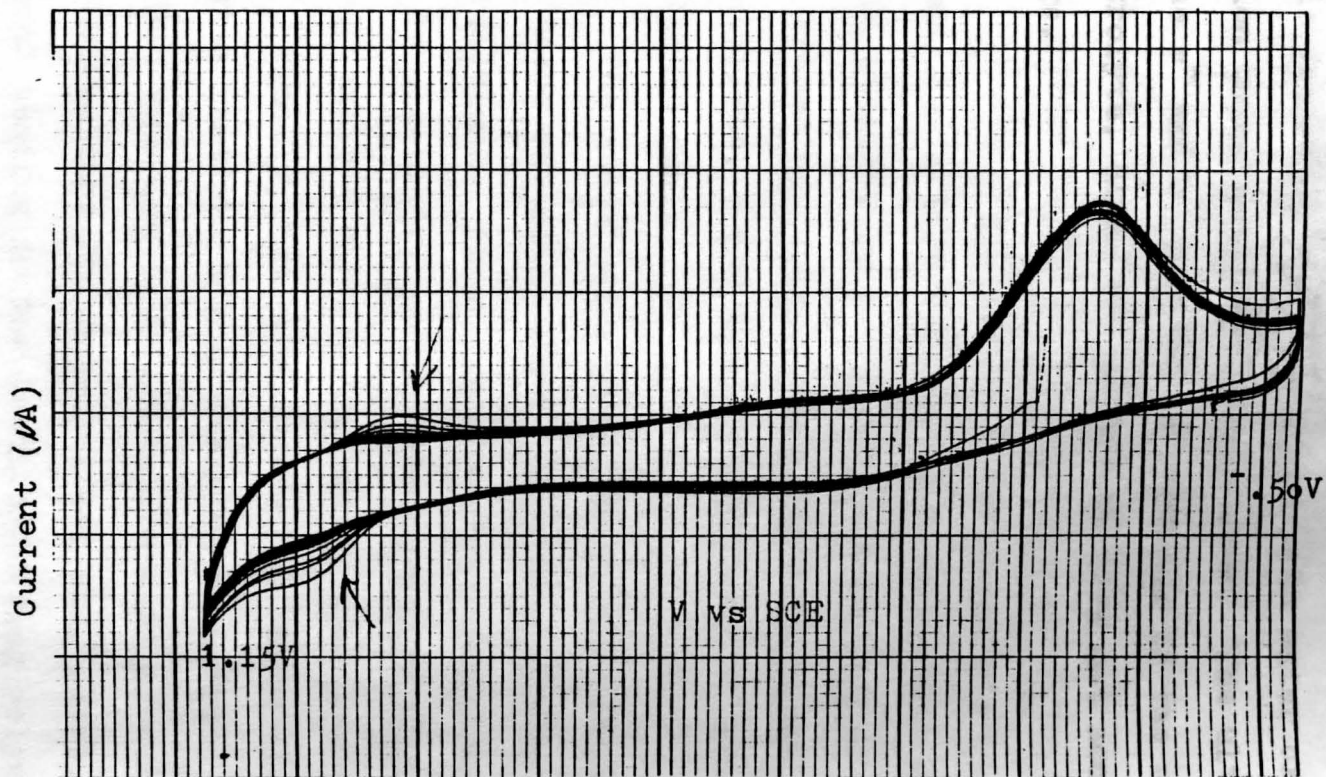


Fig. 34. CV of a poised electrode, ($+1.15\text{V}$, 2 hrs.), rinsed and then reimmersed in $.1\text{N Na}_2\text{SO}_4$. The anodic wave diminishes with time, but note the conductive layer that was there initially.

But it is not known if this layer is a poly(CH), though the observations are consistent with this possibility. Moreover, the positions of the redox waves observed when the layer is deposited are consistent with water oxidation and reduction being mediated by the layer. The ultimate origin of the e^- and h^+ for the CV currents is the supporting electrolyte, since the electrode does not accumulate trapped charge.

Since the redox waves enhanced by the deposition of this layer disappear with repeated CV scan, it is inferred that the conductive structure of this film is attacked by the redox intermediates. This, and other reasoning, suggest that the film could well be the polyacetylene, doped by GAS, that was originally sought as a synthetic goal.

The redox waves noted when the film was present, occur where one might expect the water oxidation and reduction reactions. These occur at lower voltages than for the naked Pt electrode, so that the (probably) polymeric layer seems to exhibit electrocatalysis (lower overvoltage).

Finally, the anodic currents under illumination indicates that the charge carrying structure of the film is lost when exposure to redox intermediates occur. The absence of a photovoltage indicates either very sharp, or very little, band bending in the (semiconducting polymer) layer.

Work should be done on obtaining more of a layer on the Pt electrode so that evaluation of this layer can progress. It seems that growing the conductive layer with

repeated cycling produces different kinds of films than a fixed electropolymerization.

CHAPTER V

If band bending is observed through photovoltages, the separation of

CONCLUSIONS

the following equation:

The major finding of this work is that an electroactive layer of acetylene-derivatized CAS can be electrochemically deposited on a Pt surface. Since the redox waves enhanced by the deposition of this layer diminish with repeated CV scan, it is inferred that the conductive structure of this film is attacked by the redox intermediates. This, and other reasoning, suggest that the film could well be the polyacetylene, doped by CAS, that was originally sought as a synthetic goal.

The redox waves noted when the film was present, occur where one might expect the water oxidation and reduction reactions. These occur at lower voltages than for the naked Pt electrode, so that the (probably) polymeric layer seems to exhibit electrocatalysis (lower overvoltage).

Finally, the anodic currents under illumination indicates that the charge carrying structure of the film is lost when exposure to redox intermediates occur. The absence of a photovoltage indicates either very sharp, or very little, band bending in the (semiconducting polymer) layer.

Work should be done on obtaining more of a layer on the Pt electrode so that evaluation of this layer can progress. It seems that growing the conductive layer with

repeated cycling produces different kinds of films than a fixed electropolymerization.

If band bending isn't observed through photovoltages, the separation of the e^-/h^+ isn't attained. From the following equation:

$$w = (2\epsilon\epsilon_0 V_b / qN)^{\frac{1}{2}} \quad (6)$$

where V_b is the amount of band bending in the depletion layer, N is the charge carrier density in the semiconductor, q is the electronic charge, ϵ is the dielectric constant of the semiconductor, ϵ_0 is the permittivity of free space, and w is the width of the depletion layer. The width of the depletion layer can be changed by varying the charge carriers, N , which is presumed to be the dye carrier density. This can be achieved by copolymerizing propargyl alcohol with the CAS monomer already synthesized. In semiconductors, w varies from 100°A to a few microns, and in metals, the space charge region is infinitesimally small, which is why charges induced at the electrode are maintained at the surface. 32

11. Gerischer, H., Solar Power and Fuels, Proceedings of the First International Conference on the Photoelectrochemical Conversion and Storage of Solar Energy, London, Canada, Academic Press, 1977, p. 77.
- 11b. Mettes, H.D., private communication.
12. Meler, H., Organic Semiconductors, Verlag Chemie, GmbH, 1974, Weinheim, Germany, pp. 229-230.
13. ibid.
14. ibid.
15. Rembaum, A., Encyclopedia of Polymer Science and Technology, 11, 318, 1969.

BIBLIOGRAPHY

1. Mettee, H.D., "Photoelectrochemical Catalysis with Polymer Electrodes," ACS Symposium Series, in press.
2. Watanabe, T., et al., "Electrochemical Hydrogen Production," Solar Hydrogen-Energy Systems, edited by T. Ohta, Pergamon Press Ltd., 1979, p. 137.
3. ibid.
4. Wrighton, M.S., "Conversion of Visible Light to Electrical Energy: Stable Cadmium Selenide Photoelectrodes in Aqueous Electrolytes," Solid State Chemistry of Energy Conversion and Storage, edited by J.B. Goodenough and M.S. Whittingham, American Chemical Society, Washington, D.C., 1977.
5. Janzen, A.F., "Photoelectrochemistry I-Photoelectrolysis," Solar Energy Conversion-An Introductory Course, edited by A.E. Dixon and J.D. Leslie, Pergamon Press, 1978, pp. 905-921.
6. Fujishima, A. and Honda, K., Nature, 238, 37, 1972.
7. Nozik, A.J., Applied Physics Letters, 29, 150, 1976.
8. Morrison, R.T., and Boyd, R.N., Organic Chemistry, 3rd ed., Allyn & Bacon, Boston, 1976, p. 559.
9. Dixon, A.E., "Review of Solid State Physics," Reference 5, pp. 773-784.
10. Reference 5.
11. Gerischer, H., Solar Power and Fuels, Proceedings of the First International Conference on the Photoelectrochemical Conversion and Storage of Solar Energy, London, Canada, Academic Press, 1977, p. 77.
- 11b. Mettee, H.D., private communication.
12. Meier, H., Organic Semiconductors, Verlag Chemie, GmbH, D694, Weinheim, Germany, 1974, pp. 229-230.
13. ibid.
14. ibid.
15. Rembaun, A., Encyclopedia of Polymer Science and Technology, 11, 318, 1969.

16. Hatano, M., Kambara, S., and Okamoto, S., Journal of Polymer Science, 51, 26, 1961.
17. Street, C.B., and Clarke, T.C., "Conducting Polymers: A Comparison of the Properties of Polythiazyl(SN)_x and Polyacetylene(CH)_x and Their Derivatives," Solid State Chemistry: A Contemporary Overview, edited by S.L. Holt, Advances in Chemistry Series 186, American Chemical Society, Washington, D.C., p. 178.
18. Chiang, C.K., et al., Journal of American Chemical Society, 100, 1013, 1978.
19. Young, X., et al., IUPAC 28th Macromolecular Symposium, July 12-16, 1982, Univ. of Mass., Amherst, Mass.
20. Chien, J.C., Journal of Polymer Science, Polymer Letters Edition, 19, 249, 1981.
21. Fincher, C.R., et al., Solid State Communications, 27, 489, 1978.
22. Venkataraman, V., The Analytical Chemistry of Synthetic Dyes, John Wiley & Sons Inc., 1977, p. 29.
23. Stine, K.E., Modern Practices in Infrared Spectroscopy, Beckman Instruments Inc. Fullerton, CA, 1975, Chapter 6.
24. Reference 8, pp. 672-681.
25. Silverstein, R.M., Bassler, G.C., and Morrill, T.C., Spectrometric Identification of Organic Compounds, 3rd ed., John Wiley & Sons, 1974, pp. 73-83.
26. Simons, W.W., and Zanger, M., Sadtler Guide to NMR Spectra, Sadtler Research Laboratories Inc., Philadelphia, Pa., 1972.
27. Pouchert, G., and Campbell, J., Aldrich Library of NMR Spectra, Aldrich Chemical Company Inc., 10, pp. 123-134, 1974.
28. ibid.
29. Reference 8, pp. 259.
30. Subramanian, , Advances in Polymer Science, edited by H.J. Cantow, et al., Springer Verlag, Heidelberg, 1979, pp. 33-59.
31. Anson, F.C., Analytical Chemistry, 49, 11, 1977.
32. Nozik, A.J., Annual Review of Physical Chemistry, 29, 189, 1978.